

AD _____

Award Number: DAMD17-99-1-9065

TITLE: Magnetic Resonance Studies of Photosensitizers and Their
Effect in Tumors

PRINCIPAL INVESTIGATOR: Subbaraya Ramaprasad, Ph.D.

CONTRACTING ORGANIZATION: University of Nebraska Medical Center
Omaha, Nebraska 68198-5100

REPORT DATE: August 2003

TYPE OF REPORT: Annual

PREPARED FOR: U.S. Army Medical Research and Materiel Command
Fort Detrick, Maryland 21702-5012

DISTRIBUTION STATEMENT: Approved for Public Release;
Distribution Unlimited

The views, opinions and/or findings contained in this report are those of the author(s) and should not be construed as an official Department of the Army position, policy or decision unless so designated by other documentation.

20040226 049

REPORT DOCUMENTATION PAGEForm Approved
OMB No. 074-0188

Public reporting burden for this collection of information is estimated to average 1 hour per response, including the time for reviewing instructions, searching existing data sources, gathering and maintaining the data needed, and completing and reviewing this collection of information. Send comments regarding this burden estimate or any other aspect of this collection of information, including suggestions for reducing this burden to Washington Headquarters Services, Directorate for Information Operations and Reports, 1215 Jefferson Davis Highway, Suite 1204, Arlington, VA 22202-4302, and to the Office of Management and Budget, Paperwork Reduction Project (0704-0188), Washington, DC 20503

1. AGENCY USE ONLY (Leave blank)		2. REPORT DATE August 2003	3. REPORT TYPE AND DATES COVERED Annual (15 Jul 2002 - 14 Jul 2003)	
4. TITLE AND SUBTITLE Magnetic Resonance Studies of Photosensitizers and Their Effect in Tumors			5. FUNDING NUMBERS DAMD17-99-1-9065	
6. AUTHOR(S) Subbaraya Ramaprasad, Ph.D.				
7. PERFORMING ORGANIZATION NAME(S) AND ADDRESS(ES) University of Nebraska Medical Center Omaha, Nebraska 68198-5100 E-Mail: SRAMAPRASAD@UNMC.EDU			8. PERFORMING ORGANIZATION REPORT NUMBER	
9. SPONSORING / MONITORING AGENCY NAME(S) AND ADDRESS(ES) U.S. Army Medical Research and Materiel Command Fort Detrick, Maryland 21702-5012			10. SPONSORING / MONITORING AGENCY REPORT NUMBER	
11. SUPPLEMENTARY NOTES Original contains color plates: All DTIC reproductions will be in black and white.				
12a. DISTRIBUTION / AVAILABILITY STATEMENT Approved for Public Release; Distribution Unlimited				12b. DISTRIBUTION CODE
13. ABSTRACT (Maximum 200 Words) In this project, we use specifically fluorine labeled photosensitizers which will be of utility in the treatment of breast cancer via photodynamic therapy (PDT). The accumulation of the photosensitizer in the tumor and the muscle are evaluated using noninvasive ¹⁹ F spectroscopic modality in mice bearing RIF tumor. By determining the relative disposition of the sensitizer, we can determine the best time to irradiate the tumor causing minimal damage to nearby healthy cells around the tumor. The absorption, distribution and elimination of the labeled sensitizer is achieved by ¹⁹ F spectroscopy of tumor models after administering a single dose of the sensitizer. The tumor destruction is achieved by irradiating the tumor with an appropriate wavelength laser light. The process of tumor destruction and the accompanying changes in the high energy phosphates and diffusion process are monitored by ³¹ P and ¹ H MR studies. The ³¹ P MR studies performed before and after the use of ¹⁹ F labeled PS(DoD2) does not show any appreciable changes in the spectra but tumor regression was observed after PDT studies under fractionated laser doses. The corresponding nonlabeled compound did not show ³¹ P spectra changes or tumor regression following PDT.				
14. SUBJECT TERMS ¹⁹ F NMR, ³¹ P MR, Relaxation Times, Diffusion, Photodynamic Therapy, Tumor Regression, RF coils				15. NUMBER OF PAGES 82
				16. PRICE CODE
17. SECURITY CLASSIFICATION OF REPORT Unclassified	18. SECURITY CLASSIFICATION OF THIS PAGE Unclassified	19. SECURITY CLASSIFICATION OF ABSTRACT Unclassified	20. LIMITATION OF ABSTRACT Unlimited	

Table of Contents

Cover.....	1
SF 298.....	2
Table of Contents.....	3
Introduction.....	4
Body.....	4
Key Research Accomplishments.....	9
Reportable Outcomes.....	10
Conclusions.....	10
References.....	11
Appendices.....	12

INTRODUCTION

The diagnosis and treatment of cancer is an important healthcare issue. This project is concerned with the development and monitoring of fluorine labeled photosensitizer (PS) for the treatment of breast cancer by a relatively new and evolving cancer treatment modality. The photosensitizers are new and hence can not be administered to humans directly. This necessitates the use of a suitable tumor model. Using a mouse foot tumor model, the labeled photosensitizer has been monitored over time in single subjects. The information obtained from in vivo MR studies on the rate of rate of absorption, the time of peak concentration, and the rate of elimination were used to choose the time to irradiate the tumor with laser light at appropriate wavelength. The response to PDT was measured by ^{31}P MR spectroscopy. These studies will provide information of significant value to breast cancer research and treatment via photodynamic therapy.

Body (Research accomplishments and details of the work)

Task-1

As a significant part of the study we have been able to obtain sufficient amount of fluorinated photosensitizer with 12 equivalent fluorine atoms in the porphyrin photosensitizer. This sensitizer has an absorption peak at 626nm and is effective at 10 micromole concentration in the animal model.

Task -2

PDT studies were done on both the fluorine labeled and nonlabeled compounds. Our studies have shown that PDT performed with this drug administered IP at 10 $\mu\text{M}/\text{kg}$ lead to tumor regression. Representative ^{31}P MR studies were performed on tumors both before and after the initiation of PDT. The effect of PDT on tumor volumes with each of the three photosensitizers (fluorine labeled, non labeled and photofrin) is shown in Figure 2(see page 6). The growth pattern of unperturbed tumors is also shown for comparative purpose in this figure.

Task-3

A second photosensitizer which we refer to as DoD-6 (with 6 equivalent fluorines) has been developed (with Co-I, Dr. Ravindra Pandey, Roswell Park Cancer Institute). A brief description of the synthesis of this compound is provided later (see page 8).

Details of research work

The RIF tumors used in the study were produced following the protocol of Twentyman et al (1). We studied 57 mice tumors during the past year. The growth of tumors before PDT and regression following PDT were monitored by making tumor volume measurements 4 to 5 times a week. The volumes were measured by measuring the three diameters and the volume computed using the ellipsoid approximation. The studies were performed on the fluorine labeled photosensitizer, the non labeled analog and the FDA approved photofrin. The drug was administered at a dose of 10 $\mu\text{M}/\text{kg}$. A detailed presentation of the synthesis along with mass spectroscopic and high resolution MR data was presented at the ERA of Hope meeting at Florida (2002 August). A copy of the abstract is attached in the appendix. The doubling times of tumor growth before PDT were found to be 125 mm^3 (n=9). A complete analysis of several tumor doubling times before and after therapy are documented in Table 1 (see Appendix). The tumor

regression with one PDT treatment with a single or fractioned dose was observed for a few days post therapy. No complete tumor regression was seen in a single treatment alone (Table 2, in Appendix). Tumor regression with DoD-2 was as large as 30-40% and tumor regrowth started after a few days of regression.

In order to obtain optimum time for laser irradiation and to quantitate the photosensitizer in the tumor noninvasively, we used ^{19}F spectroscopic technique to follow the labeled photosensitizer. As a first approximation we assume that the rate of absorption, retention and elimination are independent on the drug dose. At present we are able to perform these ^{19}F MR studies at a drug dose of $100\text{ }\mu\text{M/kg}$. A home built surface coil was used to perform these studies on the 7Tesla animal imager. A knowledge of the relaxation times T_1 and T_2 are necessary for optimization of the spectral data. The mean values of relaxation times in the solution were $924\pm38\text{ ms}$ for T_1 and $150\pm2\text{ ms}$ for T_2 and were used to optimize of tumor spectra. By comparing the intensities from the tumor volume with a phantom containing a known concentration of PS, the amount of PS in the tumor could be calculated. The entire Pharmacokinetic profile of PS in tumor model was constructed using three tumors (Figure 1). Based on this profile PDT was performed at time points 2hr, 4hr and 24 hrs post drug administration. The various parameters used in PDT studies are listed in Table 3.

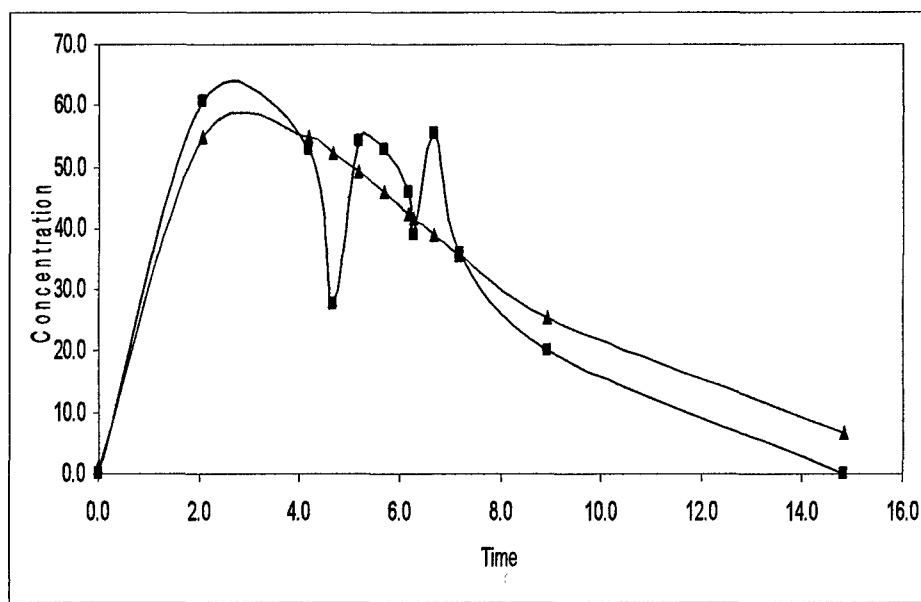


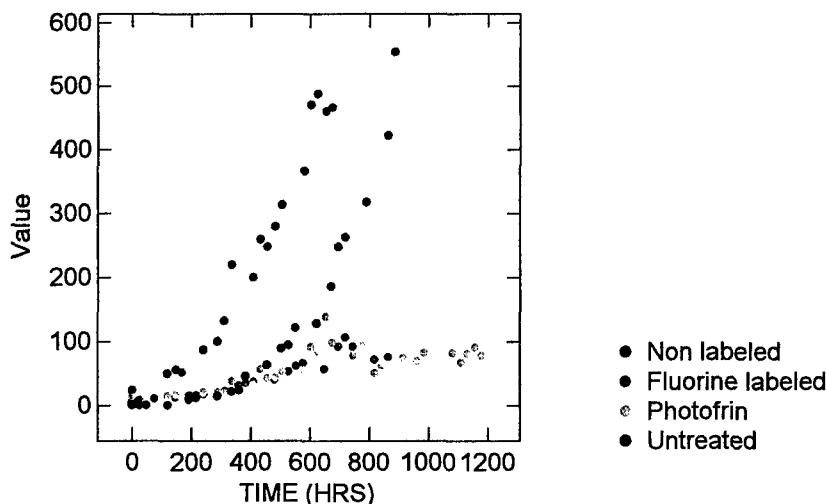
Figure 1: Pharmacokinetic profile for DoD2 in RIF tumor model. The black line connects the experimental points while the red line is the fit to the data.

The results show that this photosensitizer has fast elimination constant. The drug is eliminated completely in about 16 hours. The peak value was reached around 2 hrs. The absorption, distribution and elimination were obtained using equation

$$C = Ae^{-\alpha t} + De^{-\mu t} + Ee^{-\gamma t}$$

Where α , β and γ are the three rate constants for absorption, distribution and elimination phases. The analysis was done using the PK solutions software (7).

Figure 2



Using this information from in vivo ^{19}F MR studies, several mice tumors were studied for PDT effects using the fluorine labeled and nonlabeled analog. A typical growth plot of unperturbed tumor and a representative graph indicating the PDT effects on the tumor volumes upon using DoD-1, DoD-2 and photofrin are shown in Figure 1. Under similar doses of photofrin and DoD-2 tumors showed regression pattern similar to DoD-2. The data shown in Figure 1 clearly demonstrates this (see the data shown in green and sea blue colors for photofrin and DoD-2). DoD-1 did not exhibit any tumor regression in the studies performed so far (data in red). Thus, under the assumption that the pharmacokinetics for the labeled compound is similar to that of the labeled compound, it appears that the PDT efficacy for the non labeled compound is very small or negligible. This certainly demonstrates that the properties of fluorine labeled photosensitizer has significantly different efficacy in this case.

The laser energies used in the study were optimized at $10\mu\text{M/kg}$ dose of the PS. The laser power was at 75 or 150 mW/cm^2 at the surface of the tumor and the irradiation time was 30 minutes. In some cases, at the higher power of 150 mW/cm^2 , laser irradiation was performed for two 30 minutes duration separated by a time interval of 2 hours. The results are summarized in Table 1(see appendix). It may be noted that tumor regression was more pronounced with the administration of fractionated doses of laser.

Our results so far show that both DoD-2 and photofrin show very similar response (see Figure 1). However the non labeled PS did not show any tumor regression at any of the above mentioned laser powers.

^{31}P MR studies

Phosphorus -31 MR studies were performed using a home built ^{31}P coil (diameter 1.5 cm) operating at 121.6 MHz.

The ^{31}P MR spectra were recorded for treated untreated tumor and were used as reference spectra. For each tumor that was subject to PDT using one of the photosensitizers, a control ^{31}P MR spectrum was recorded followed by ^{31}P spectra after PDT. Our results show that the ^{31}P spectra recorded post PDT using either DoD-1 or DoD-2 do not show any measurable changes in the first few hours. Photofrin, on the other hand has shown measurable decreases in ATP peaks and a concomitant increase in Pi (inorganic phosphate peaks) (2-6). The spectral analyses were done using the JMRUI software and a typical spectral deconvolution is shown below.

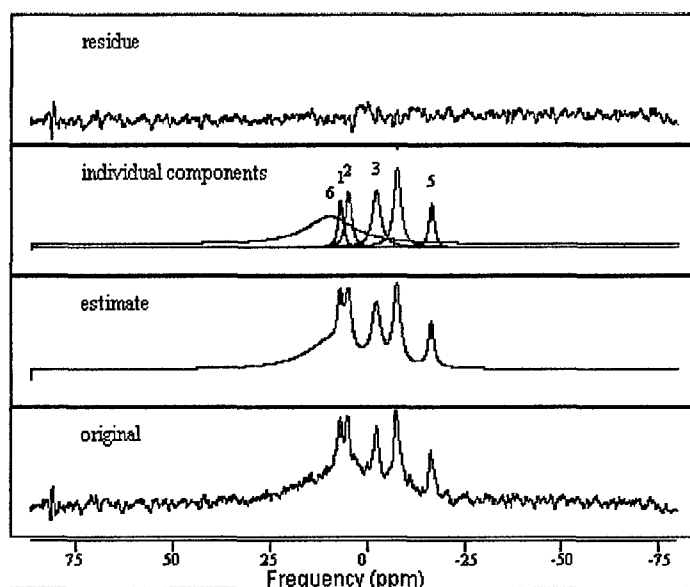


Figure 3: Typical fit to a tumor ^{31}P spectrum performed using the MRUI program. The peak assignments are: 1. PME, 2. Pi, 3. γATP , 4. αATP 5. βATP and 6. A hump arising mostly from immobile phosphorus such as bone.

Although both DoD-1 and DoD-2 did not show any changes in ^{31}P spectra, tumor administered with DoD-2 showed tumor regression. Further analysis and its relevance to functioning of photosensitizers are under way by our team. We also plan to extend our studies to beyond 4-6 hours. These results can provide more information about the function of the photosensitizer and aid in the construction of more potent and efficient photosensitizer.

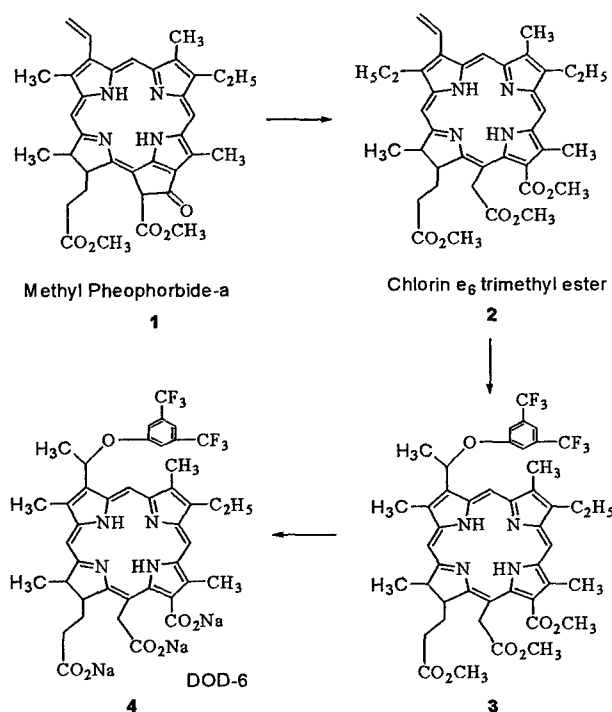
As suggested in our original statement of work we have now developed a second photosensitizer. The synthesis was done by Dr Ravi Pandey and co-workers at Roswell park cancer Institute.

Preparation of Fluorinated Chlorin

Methyl pheophorbide-a **1** was converted into chlorin e_6 trimethyl ester **2** by following the literature procedure and was isolated in >75% yield. The intermediate unstable bromoderivative obtained by reacting **2** with 30% HBr/acetic acid was dried under vacuum and immediately

reacted with 3,5-bis-(trifluoromethyl)benzyl alcohol. The resulting product obtained after the standard work-up was purified by Alumina (Gr III) column chromatography, eluting with dichloromethane. The appropriate fractions were combined. Evaporation of the solvent gave **3** in 72% yield. The methyl ester functionalities were then hydrolyzed with aqueous sodium hydroxide/THF/methanol and the reaction was monitored by HPLC analysis. After the completion of the reaction the solvents were evaporated under high vacuum. The reaction product was redissolved in phosphate buffer and the pH of the solution was adjusted to 7.4.

The structures of the intermediates (see figure 4) and the final product were confirmed by NMR and mass spectrometry analyses.



Scheme 1

Figure 4

MR studies of DOD6 (newly synthesized 2nd photosensitizer)

This photosensitizer has a strong absorption maximum at 650 nm. Because of the higher wavelength we can expect better penetration in the tissue. We have performed relaxivity measurements using the in vivo MR imager at 7T. The T_1 measurements were performed using the saturation recovery method and the T_2 measurements were done using the Hahn spin echo technique. The mean T_1 and T_2 values are ~250 and ~25 ms respectively.

We are now in the process of observing this in the tumor and the tissue. These studies are just underway in our laboratory.

The preliminary PDT studies have been performed using laser power of 150 mW/cm² and photosensitizer dose of 10 mg/kg. Interestingly the tumor regression was observed approximately two days after the initiation of the therapy.

In our laboratory here at Nebraska, we have tested the efficacy of this compound in the mouse tumor model. An example of this is shown below where the tumor volume is plotted against time.

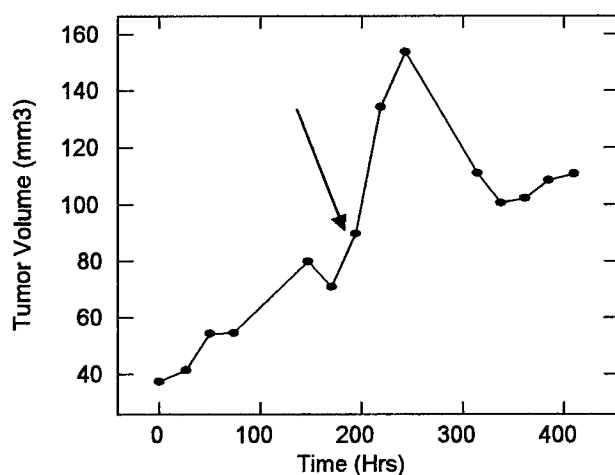


Figure 5: The growth pattern of RIF tumor before and after the PDT. The red arrow indicates the time of laser irradiation.

Key Research Accomplishments

- Using ¹⁹F MR spectroscopic method, the entire pharmacokinetic profile of the compound was generated (A copy of the abstract is enclosed in the Appendix).
- ³¹P MR spectra of tumors were studied before and after the initiation of PDT.
- PDT studies were performed using laser light at 630 nm, 270 joules/cm energy. The time point was chosen to represent maximum concentration of the photosensitizer as obtained from the pharmacokinetic data obtained in our study.
- The photosensitizer DoD2 showed tumor regression while the nonlabeled (DoD1) did not show any tumor regression. The incorporation of fluorine in the PS appears to have a positive effect on the function of the photosensitizer

Reportable Outcomes

1. Abstract of the presentation made at the ERA of HOPE meeting held at Orlando, Florida during September 25-28, 2002.
2. Abstract of the Talk to be presented at the ESMRMB meeting to be held at Rotterdam, Netherlands, during September 18-21, 2003.
3. Copy of the Abstract submitted for consideration to the SPIE international symposium to be held in San Diego, Feb 14-19, 2004.
4. A revised copy of the scientific paper related to synthesis, mass spectroscopic and in vivo ^{19}F MR studies—submitted to Tetrahedron

Funding applied for during the past two years in this or related area

1. DOD undergraduate research grant- submitted in year 2002. The proposal was not funded. A resubmission was not done as this category of research is not open for consideration in the year 2003 by DoD.
2. A grant application to Nebraska state was made in the early 2003 but was not funded. A resubmission in early 2004 will be done.

Conclusions:

Our studies demonstrate the fluorine labeled compound can be noninvasively monitored in the tumor and muscle by ^{19}F magnetic resonance spectroscopy. The ^{31}P spectroscopic data on tumors show that even though the ^{31}P spectra after PDT do not undergo significant changes the tumor shows regression. The tumor regression and the underlying mechanism of PS function will also be explored in the coming year.

It is possible to produce larger amounts of the labeled compounds for further detailed studies on the distribution in the animal and also in the tumor. The ability to monitor the fluorine labeled PS in the animal model will provide useful data before PDT is performed. In vivo MR will be a useful method in the development of new photosensitizers

References

1. Twentyman PR, Brown JM, Gray JW, Frank AJ, Scoles MA, Kallman RF. A new mouse tumor model system(RIF-1) for comparison of end point studies. *J. Natl. cancer Inst.*, 1980, 64, 595-604.
2. T L Ceckler, R.G. Bryant, D P Penney, S L Gibson and Hilf R, ^{31}P NMR spectroscopy demonstrates decreased ATP levels in vivo as an early response to photodynamic therapy, *Biochem. Biophys. Res. Commun.*, 140, 273-279, 1986.
3. S Naruse, Y Horikawa, C Tanaka, T Higuchi, H Sekimoto, S Ueda, and K. Hirakawa, Evaluation of the effects of photoradiation therapy on brain tumors with in vivo ^{31}P MR spectroscopy, *Radiology.*, 160, 827-830, 1986.
4. M. Chopp, H. Farmer, F.Hetzel and A P Schaap. In vivo ^{31}P NMR spectroscopy of mammary carcinoma subjected to subcurative photodynamic therapy, *Photochem. Photobiol.* 46, 819- 822, 1987.
5. R Hilf, S L Gibson, D P Penney, T.L. Ceckler, R G Bryant, Early biochemical responses to photodynamic therapy monitored by NMR spectroscopy. *Photochem. Photobiol.* 46, 809-817. 1987.
6. S Ramaprasad, R K Pandey, R.M. Hawk, Y.H. Liu. Responses to Photodynamic therapy in a murine tumor model-- ^{31}P NMR and water proton relaxation studies, *J. Environ. Sci. Health. A28*, 2345-2357. 1993.
7. PK Solutions Software (version 2.0), Summit Research Services, Colorado, 2001

Appendix-A

**Copy of the research results in the form of tables
Relevant to reported material**

Table 1
Tumor doubling times* for various PDT treated and untreated tumors.

Cage & Mouse	Drug used	Tumor treatment	Tumor Doubling Time (Hr)
C5M1	DOD1	PDT treated	173.3
C5M2	DOD1	PDT treated	115.5
C5M3	DOD1	PDT treated	115.5
C10M1	DOD2	PDT treated	173.3, 693.1
C10M3	DOD2	PDT treated	115.5, 231.0 693.1
C10M5	DOD2	PDT treated	173.3 231.0 173.3
C7M3	None	untreated	77.0
C7M4	None	untreated	69.3
C8M4	None	untreated	115.5
C8M1	Photofrin	PDT treated	173.3 693.1
C12M2	Photofrin	PDT treated	173 231

Note: In doubling time calculation is based on following segs.

C10M1: seg1 (ascending, March 24-April 17, 03), seg3 (descending, April 25-May 5, 03).

C10M3: seg1 (ascending, March 24-April 17, 03), seg2 (descending, April 17-21, 03), seg3 (ascending, April 23-May 5, 03).

C10M5: seg1 (ascending, March 24-April 24, 03), seg2(descending, April 24-30, 03), seg3 (ascending, April 30-May 19, 03).

C8M1: seg1 (ascending, Dec. 23, 02 – Jan. 17, 03), seg2(descending, Jan. 20-29, 03), no seg3.

C12M2: seg1 (ascending, May 23-June 19, 03), doubling time is 173.3. If taking all points after peak (June 19-July 11, 03), including peak, the doubling time (DT) is 693.1. After taking peak point and five points following it (June 19-June 27, 03), DT is 231.

* The term “doubling times” is used to define the increase or decrease in tumor volumes. The values corresponding to ascending or descending phases of the tumor growth refers to increasing or decreasing volumes of the tumor.

Table 2
Tumor regression after PDT with DOD1 and DOD2 photosensitizers

Cage & Mouse #	Drug used and Dose	Tumor vol (day of PDT)	Laser 1 Power	Laser 2 Power	Remarks
C5 M1	DOD1 0.35ml	458.76	135 Joules	-----	No real tumor regression seen
C5 M2	DOD1 0.33ml	148.82	135 Joules	-----	No real tumor regression seen
C5 M3	DOD1 0.33ml	487.03	135 Joules	-----	No real tumor regression seen
C12 M5	DOD1 0.7ml	131.78	270 Joules	-----	No real tumor regression seen
C13 M2	DOD1 0.565ml	65.54	270 Joules	270 Joules	A little tumor regression seen
C13 M4	DOD1 0.649ml	107.86	270 Joules	270 Joules	No real tumor regression seen
C4 M3	DOD2 0.43ml	271.73	135 Joules	-----	No real tumor regression seen
C4 M4	DOD 2 0.42ml	245.2	135 Joules	-----	No real tumor regression seen
C10 M1	DOD2 0.96ml	179.22	270 Joules	-----	A very slight tumor regression 4 days after irradiation
C10 M3	DOD2 10uM	391.18	270 Joules	-----	Some Tumor regression on days 1-4 after irradiation
C01 M4	DOD2 0.6ml	150.37	135 Joules	-----	No real tumor regression seen
C10 M5	DOD2 0.92ml	106.32	270 Joules	270 Joules	Tumor regression seen for 8 days after irradiation
C11 M1	DOD2 0.84ml	83.18	270 Joules	-----	A slight tumor regression 3 days after irradiation
C11 M2	DOD2 0.81ml	63.38	270 Joules	-----	No real tumor regression seen
C11 M3	DOD2 0.60ml	70.78	270 Joules	270 Joules	Regression seen the day after irradiation

Table 3
The laser power, duration of irradiation used in our PDT studies

Univ. #	Mice # (Cage #, ear notch #)	P.S. Admin.	Date of irradiation	Duration Of irradiation	Irradiation time post PS injections	Power used	Total incident energy (joules)
18	C4 M3	DOD 2 .43 ml	10/10/02	30 minutes	24 hours	75mW	135
19	C4 M4	DOD 2 .42 ml	10/10/02	30 minutes	24 hours	75mW	135
21	C5 M1	DOD 1 .35 ml	10/10/02	30 minutes	24 hours	75mW	135
22	C5 M2	DOD 1 .33 ml	10/10/02	30 minutes	24 hours	75mW	135
23	C5 M3	DOD 1 .33 ml	10/10/02	30 minutes	24 hours	75mW	135
26	C6 M1	Photofrin .245 ml	10/4/02	10 minutes	24 hours	225-230 mW	135
27	C6 M2	Photofrin .235 ml	10/4/02	10 minutes	24 hours	225-230 mW	135
28	C6 M3	Photofrin .240 ml	10/4/02	10 minutes	24 hours	225-230 mW	135
29	C6 M4	Photofrin .265 ml	10/4/02	10 minutes	24 hours	225-230 mW	135
30	C6 M5	Photofrin .260 ml	10/4/02	10 minutes	24 hours	225-230 mW	135
36	C8 M1	Photofrin 25mg/kg	1/15/03	30 minutes	24 hours	75mW	135
41	C9 M1	DoD2 3mg	3/20/03	30 minutes	24 hours	150mW	135
44	C9 M4	Photofrin .24 ml	3/12/03	30 minutes	24 hours	75 mW	135

Appendix-B

Copy of the Abstracts and the Paper

**SYNTHESIS AND IN VITRO PHOTSENSITIZING
EFFICACY OF FLUORINATED PORPHYRIN-
BASED PHOTSENSITIZERS FOR IN VIVO
MR STUDIES**

**Suresh K. Pandey, Amy L. Gryshuk, Andrew Graham,
Allan Oseroff, S. Ramaprasad,¹
and Ravindra K. Pandey**

Photodynamic Therapy Center, Roswell Park Cancer
Institute, Buffalo, NY 14263 and ¹Department of
Radiology, Nebraska Medical Center, Omaha, NE 68198

ravindra.pandey@roswellpark.org and
sramaprasad@unmc.edu

In vivo MR spectroscopy has been used increasingly to monitor metabolism and disease states in humans. Both magnetic resonance imaging and spectroscopy have evolved into sophisticated diagnostic techniques. In addition to the proton, nuclei such as fluorine can be studied by in vivo spectroscopy and imaging. Fluorine-19 NMR is a technique with significant potential because of the relatively high sensitivity and low endogenous background. Fluorine-19 MR has been used to study metabolism, tumor growth, and blood flow. MR of fluorinated compound is particularly attractive for in vivo studies of human and animal models. The F-19 isotope has a 100% natural abundance, a spin of 1/2, and an MR sensitivity that is 83% that of hydrogen.

To date, most of the fluorinated porphyrin-based analogs synthesized for in-vivo F-19 NMR studies have been unsymmetrical, and thus lead to signal dispersion. In order to have strong fluorine signal at a low concentration of the drug in tumor, it is necessary to have photosensitizers containing multiple fluorine units. It would be advantageous to have a center of symmetry in the fluorinated photosensitizer that will render the fluorine nuclei to be equivalent and provide signal addition of all equivalent nuclei. We have succeeded in synthesizing porphyrins containing six to 12 symmetrical fluorines. These compounds were prepared in multi-step syntheses. The structures were confirmed by NMR, mass spectrometry and elemental analyses. The symmetry of the fluorines was confirmed by F-19 NMR studies. Compared to the non-fluorinated analogs, the fluorinated porphyrins showed enhanced singlet oxygen producing efficiency.

The in-vitro photosensitizing efficacy of the fluorinated porphyrins was investigated in RIF tumors at various doses and showed promising activity. The synthesis, photophysical characteristics and in-vitro photosensitizing results of the newly synthesized fluorinated porphyrin-based compounds will be discussed.

Accepted for Oral Presentation at the European Society of Magnetic Resonance in Medicine in Rotterdam, Netherlands, September 2003.

In Vivo ^{19}F MR Studies of Fluorine Labeled Photosensitizer in Murine Tumor Model

S. Ramaprasad¹, E. Rzepka¹, S.S. Joshi², M. P. Dobhal³, J. Missert³, R.K. Pandey³

¹Department of Radiology, University of Nebraska Medical Center, Omaha, NE, U.S.A

²Departments of Genetics, Cell Biology, and Anatomy, University of Nebraska Medical Center, Omaha, Nebraska, U.S.A. ³Photodynamic Therapy Center, Roswell Park Cancer Institute, Buffalo N.Y, U.S.A.

Introduction

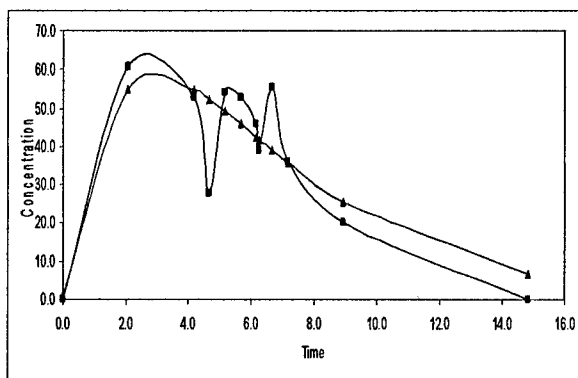
Photodynamic therapy (PDT) is a cancer treatment modality that combines light sensitive drug and lasers [1]. Monitoring the photosensitizer (PS) in the tumor and in normal tissue is helpful in the development of new photosensitizers. Syntheses of labeled photosensitizer that can be monitored by MR studies offer the advantage of noninvasive assessment of the photosensitizer in a single subject [2]. The assessment of the same in the skin and underlying muscle may provide information about the cutaneous toxicity of PS. In this work we present the construction of pharmacokinetic profile of a new photosensitizer in a tumor model and its utility in PDT studies.

Methods

The Radiation induced fibrosarcoma (RIF) cells were maintained according to the protocol of Twentyman et al [3]. Tumors were grown on mouse foot dorsum by inoculating 2×10^5 cells. The photosensitizer was administered IP ($\sim 100 \mu\text{M}$). ^{19}F MR spectra were collected on a Bruker 7T instrument using a home built surface coil. The ^{19}F MR spectral parameters included a 90° pulse of $16 \mu\text{s}$, a spectral width of 20 KHz, 8K data points, and a 2s repetition time for a total accumulation time of 30 minutes. PDT measurements were performed at 630 nm with an argon ion (Spectra physics model 2045) pumped dye laser (Spectra Physics, 375B). Laser irradiation was done for 30 minutes at a power of 150 mW cm^{-2} leading to a total light dose of 270 J cm^{-2} .

Results

In this presentation we report the results obtained using a newly synthesized water



soluble form of fluorine labeled photosensitizer which was monitored in mouse tumor model over time. The measured relaxation times in the solution were $924 \pm 38 \text{ ms}$ for T_1 and $150 \pm 2 \text{ ms}$ for T_2 and were used to optimize of tumor spectra. The Pharmacokinetic profile of PS in tumor model was constructed using three tumors (Figure 1). Based on this

profile PDT was performed at time points 2hr, 4hr and 24 hrs post drug administration.

Conclusions:

MR studies can provide quantitative data on photosensitizer in tumor and a rational basis for PDT initiation. PDT studies done at 2hrs post PS administration led to tumor regression between days 2-4.

References

1. Dougherty, TJ, et al. [1998] J.Natl. Cancer. Inst. 41:351-359.
2. Ramaprasad et al [1994] Proc. Soc.Magn. Reson Med. 3: 1348.
3. Twentyman et al [1980] J.Natl. Cancer. Inst.64: 595-604.

Acknowledgement

This research was funded by the Department of Defense (DAMD 17-99-1-9065).

Submitted to SPIE's International Symposium on Medical Imaging 2004.
(San Diego, CA)

ABSTRACT

The changes in the tumor that occur following photodynamic therapy (PDT), a cancer treatment modality, were studied using a small animal MR imager operating at 7Tesla. The animal model used in these studies was mice implanted with radiation -induced fibrosarcoma (RIF). The tumor bearing mice were injected with 10 μ M/kg of one of the three photosensitizers: 1) Photofrin 2) Fluorine labeled photosensitizer and 3) Non-labeled analog of the fluorine labeled sensitizer. Laser light at 630 nm (150 mW/cm², 270 joules/ cm²) was delivered to the tumor at 2-24 hours of photosensitizer administration. The MR spectroscopic and imaging examination of the tumors involved both the ¹H and ³¹P nuclei. The tumor bioenergetics was measured by ³¹P spectroscopy. The water proton relaxivity and diffusion measurements are used to obtain local changes in different regions of the tumor.

Significant changes in ³¹P MR spectra were observed using photofrin while no statistically significant changes were observed when the fluorine labeled or its non labeled analogs were used. The PDT induced changes in tumor volumes (as measured by calipers) showed significant tumor regression with photofrin followed by moderate regression with the fluorine labeled PS and no regression with the non labeled PS. The growth pattern of tumors using nonlabeled photosensitizers followed the general pattern of unperturbed tumors. The possible relationship between the function of these sensitizers and the various MR derived parameters that characterize the tumor status will be discussed.

Authors

1. Subbaraya Ramaprasad
Department of Radiology
University of Nebraska Medical Center
Omaha, Nebraska 68198-1045
Phone: 402-559-6990 Fax: 402-559-1011
E-Mail: Sramaprasad@unmc.edu
2. Elzbieta Rzepka
Department of Radiology
University of Nebraska Medical center
Omaha, Nebraska 68198-1045
Phone: 402-559-3864 Fax: 402-559-1011
E-Mail: erzepka@mail.unomaha.edu
3. Jiaxiong Pi
Department of Radiology
University of Nebraska Medical Center
Omaha, Nebraska 68198-1045
Phone: 402-559-3865 Fax: 402-559-1011
E-Mail: jpi@mail.unomaha.edu
4. Shantaram Joshi
Department Genetics, Cell Biology and Anatomy
University of Nebraska Medical Center
Omaha, Nebraska 68198-1045
Phone: 402-559-4165 Fax: 402-559-7328.
E-Mail: ssjoshi@unmc.edu
5. Ravindra Pandey
PDT Center
Roswell Park Cancer Institute
Buffalo, New York 14263
Phone: 716-845-3203 Fax: 716-845-8920
E-Mail: Ravindra.Pandey@RoswellPark.org
6. Mahabeer Dobhal
PDT Center
Roswell Park Cancer Institute
Buffalo, New York 14263
Phone: 716-845-3203 Fax: 716-845-8920
E-Mail
7. Joseph Missert
PDT Center

Roswell Park Cancer Institute
Buffalo, New York 14263
Phone: 716-845-3377 Fax: 716-845-8920
E-Mail: JMIssert@Buffalo.com

**Fluorinated Photosensitizers: Synthesis, Photophysical, Electrochemical,
Intracellular Localization, *In-Vitro* Photosensitizing Efficacy and
Determination of Tumor-Uptake by ^{19}F *In-Vivo* NMR Spectroscopy**

Suresh K. Pandey,¹ Amy L. Gryshuk,¹ Andrew Graham,² Kei Ohkubo,³

Shunichi Fukuzumi,^{3*} Mahabeer P. Dobhal,^{1,#} Gang Zheng,¹ Zhongping Ou,⁴ Riqiang Zhan,⁴

Karl M. Kadish,^{4*} Allan Oseroff,² S. Ramaprasad,⁵ and Ravindra K. Pandey^{1,6*}

¹Photodynamic Therapy Center, ²Department of Dermatology, ⁶Department of Nuclear Medicine, Roswell Park Cancer Institute, Buffalo, NY 14263, USA.

³Department of Material and Life Science, Graduate School of Engineering, Osaka University, CREST, Japan Science and Technology Corporation (JST), Yamada-oka, Suita, Osaka 565-0871, Japan.

⁴Department of Chemistry, University of Houston, Houston, TX 77204-5003, USA.

⁵Department of Radiology, University of Nebraska, Omaha, Nebraska, USA

On leave from the Department of Chemistry, University of Rajasthan, Jaipur 302004, India

Addresses for correspondence:

Ravindra.pandey@roswellpark.org

Sramaprasad@unmc.edu

Kkadish@uh.edu

Fukuzumi@ap.chem.eng.osaka-u.ac.jp

Abstract

For *in vivo* NMR studies, starting from pyrroles, a series of fluorinated porphyrins were synthesized by following the MacDonald reaction conditions. Upon reaction with osmium tetroxide, a fluorinated porphyrin containing four trifluoromethyl groups (12 fluorine units) was converted into the related chlorin and bacteriochlorin which exhibited long-wavelength absorptions at 652 and 720 nm, respectively. All compounds produced good singlet oxygen production efficiency. A comparative study of nine porphyrins with and without fluorine substituents indicated no adverse effects of the presence of fluorinated groups in the photophysical properties of the porphyrins, chlorins or bacteriochlorins. The first and second one-electron reduction potentials (vs. SCE) of the investigated compounds range between -1.29 and -1.49 V and between -1.66 and -1.84 V in PhCN containing 0.1 M TBAP. UV-visible spectroelectrochemical data suggested the formation of π -anion and π -cation radicals upon the first reduction and first oxidation. The *in vivo* ^{19}F MR study of a representative fluorine labeled compound with twelve equivalent fluorines confirmed the presence of the fluorine labeled sensitizer in mouse (C3H/HeJ) implanted with RIF tumors in one of the hind feet. The studies performed on mice tumors ($n = 4$) confirmed the feasibility and reproducibility of *in vivo* studies. All fluorinated compounds were found to be quite effective *in vitro*. In a comparative intracellular localization study with Rhodamine-123 in RIF tumor cells, the most soluble porphyrin containing two propionic ester side chains was found to localize in mitochondria as well as the related chlorin and bacteriochlorin.

Introduction

Photodynamic Therapy (PDT) is now a well recognized modality that has been used both independently and in conjunction with other cancer treatments.¹ Combining the use of a light-sensitive drug, lasers and fiber-optic probes, PDT has emerged as one of the promising strategies in cancer treatment. In this therapy, patients are given intravenous injections of a drug that accumulates in cancer cells in much higher concentrations than in normal cells. Laser light with an appropriate wavelength delivered by fiber optics to these tumor sites produces highly reactive oxygen species (e. g. $^1\text{O}_2$) that destroy the tumor cells.² Therefore, for a drug to be effective, it is necessary that the compound be in high concentration in tumor cells. PDT is most beneficial when laser light is delivered at a time point when the photosensitizer's concentration is greater in the tumor than in the surrounding tissue. Thus, a comprehensive knowledge of the extent of localization and the rate of accumulation is of immense value. While the photosensitizer's concentration in tissue may be determined by chemical extraction techniques, these methods are invasive, time consuming, and clinically non-feasible. In contrast, *in vivo* NMR is minimally invasive, considered safe, and the therapy can be monitored over time in a single living system.³

In vivo MR spectroscopy has been used increasingly to monitor metabolism and disease states in humans. Both magnetic resonance imaging and spectroscopy have evolved into sophisticated diagnostic techniques. In addition to the proton, nuclei such as fluorine⁴ can be studied by *in vivo* spectroscopy and imaging. Fluorine-19 (^{19}F) NMR is a technique with significant potential because of the relatively high sensitivity and low endogenous background. Due, in part, to its high MR sensitivity, fluorine has received considerable attention as an MR nucleus. Fluorine-19 MR has been used to study metabolism, tumor growth, and blood flow.⁵ More recently, *in vivo* ^{19}F MR has been used to measure tumor integrity and vasculature in subcutaneously implanted

tumors in rats⁶. MR of fluorinated compounds is particularly attractive for *in vivo* studies of human and animal models. The ¹⁹F isotope has a 100% natural abundance, a spin of 1/2, and a MR sensitivity that is 83% then that of hydrogen⁷.

To date, most of the fluorinated porphyrin-based analogs synthesized for *in vivo* ¹⁹F NMR studies have been unsymmetrical,⁸ and thus lead to signal dispersion. In order to have a strong fluorine signal at a low concentration of the drug in tumor, it is necessary to have photosensitizers containing multiple fluorine units. It would be advantageous to have a photosensitizer with equivalent fluorine substituents that will render signal addition of all equivalent nuclei.

In this manuscript we report the synthesis of a series of fluorinated and the corresponding non-fluorinated porphyrin-based compounds, the effect of the substituents on their photophysical and electrochemical characteristics, their intracellular localization and their *in vitro* photosensitizing efficacy.

Results and Discussion

Chemistry. For the synthesis of porphyrin-based fluorinated photosensitizers, our synthetic strategy was divided into two parts. These were the (a) synthesis of porphyrins **1** and **2** containing symmetrical trifluoromethyl groups (total fluorine: 6) introduced at the *meta*- or *para*-position(s) of the phenyl ring and (b) porphyrins **3** and **4** bearing symmetrical trifluoromethyl groups introduced at the 3 and 5-positions (total fluorine: 12) of the phenyl ring present at the *meso*-position of the porphyrin ring system (see chart 1).

Porphyrins **1**- **4** were synthesized from pyrroles **5**,⁹ **15**¹⁰ or **19**¹¹ by following the well established "2 + 2" reaction approach¹² (see Scheme 1). In brief, reactions of pyrrole **5** with *p*-, *m*- or 3', 5'-dimethoxyphenyl aldehyde under acidic reaction conditions produced the corresponding

dipyrromethanes **6**, **7** and **8** in 60-80% yield, which on refluxing with ethylene glycol/KOH gave the related α -free dipyrromethanes **9**, **11** and **13** respectively in >85% yield. Further reaction of these dipyrromethanes with POCl₃/DMF under Vilsmeier's reaction conditions¹³ produced the corresponding diformyl dipyrromethanes **10**, **12** and **14** in excellent yields (>75%). For the preparation of dipyrromethane **17**, pyrrole **15** was first converted into the acetoxy derivative **16**, which on treating with K-10 clay¹⁴ in dichloromethane at room temperature gave the desired dipyrromethane in 70% overall yield. Reaction of pyrrole **19** with bromine/methanol¹⁵ gave the corresponding dipyrromethane **20** in 72% yield. Hydrogenation of dipyrromethane **17** and **20** in presence of Pd/C at room temperature produced the corresponding carboxylic acids **18** and **21** in quantitative yields.

Chart 1, Scheme 1

Diformyldipyrromethanes **10**, **12** and **14** were then individually reacted with dipyrromethane dicarboxylic acid **18** under McDonald reaction conditions.¹² After purification porphyrins **22-24** were isolated in modest yield. By following a similar approach, pyrromethane **14** was also reacted with pyrromethane dicarboxylic acid **21**, and porphyrin **25** was obtained in 38% yield. For the preparation of fluorinated analogs, porphyrins **22-25** containing methoxy groups in the phenyl rings were reacted with boron tribromide and the related hydroxy-phenyl porphyrins **26-29** were obtained in 70-77% yields. Further reaction of these porphyrins with 3,5-trifluoromethyl-benzyl bromide produced the desired fluorinated porphyrins **1-4** in modest yield. Reaction of **29** with 3,5-dimethyl-benzyl bromide produced the non-fluorinated porphyrin **4a** in good yield. The structures of the intermediates and the final products were confirmed by ¹H, ¹⁹F NMR, mass spectrometry and elemental analyses.

Scheme 2 and Scheme 3

Among the fluorinated porphyrins 1-4, compound 4, containing two propionic ester functionalities at the bottom half of the molecule showed enhanced solubility in 1% Tween 80/water formulation as well as improved *in vitro* photosensitizing efficacy in comparison to the other analogues. Therefore, for investigating the photosensitizing effect(s) of fluorinated groups in long-wavelength absorbing compounds, porphyrin 4 was reacted with osmium tetroxide (OsO_4) and the corresponding *vic*-dihydroxy chlorin 30 (λ_{max} : 648 nm) and tetra-hydroxy-bacteriochlorin 31 (as an isomeric mixture, λ_{max} : 716 nm) were synthesized. The yield of the individual product was found to depend on the amount of OsO_4 used.

As expected, the ^{19}F NMR spectra of all the fluorinated porphyrins 1-4 exhibited a single peak at δ 13.0 ppm due to the presence of a center of symmetry in the molecule, whereas chlorin 30 and bacteriochlorin 31 showed two peaks with equal intensity at 12.98 and 12.99 ppm respectively.

In vivo ^{19}F MR spectral characteristics. A typical ^{19}F MR spectrum of the fluorinated photosensitizer in the mouse foot tumor (volume=0.18ml) recorded on a 7T animal imager 8.0 hrs post IP administration of the compound (100 $\mu\text{M}/\text{kg}$) is shown in Figure 1. The ^{19}F MR spectral parameters included a 90° pulse of 16 μs , a spectral width of 20 KHz, 8K data points, and a 2s repetition time for a total accumulation time of 60 minutes. The ability to observe the photosensitizer by ^{19}F MR noninvasively is an important step towards understanding its pharmacokinetic characteristics and relating these to its *in vivo* photosensitizing efficacy. These details will be published elsewhere.

Figure 1

Photophysical Properties. A typical fluorescence spectrum of fluorinated porphyrins in PhCN is shown in Figure 1. For the case of 3 which exhibits virtually the same fluorescence maxima at 628 and 693 nm was observed as for non-fluorinated porphyrins. The absorption and

fluorescence maxima of investigated porphyrins **1-4**, **26-29**, chlorin **30** and bacteriochlorin **31** are listed in Table 1. The absorption and fluorescence maxima are red-shifted in order: porphyrin, chlorin and bacteriochlorin, but they are not affected by the fluorine substituents.

Table 1, Figure 2

The fluorescence decay of **3** is fitted well by a single exponential line with lifetime of 18.5 ns as shown in Figure 3. The fluorescence lifetimes are also listed in Table 1. The fluorescence lifetimes (τ) are also unaffected by fluorinated substituents. The τ values of the nine porphyrins in this table are all similar in the range of 16.1–18.6 ns irrespective of substituents, but they are significantly longer than those of chlorin **30** (3.8 ns) and bacteriochlorin **31** (3.3 ns).

Figure 3

Phosphorescence spectra were observed in deaerated frozen 2-MeTHF at 77 K. The phosphorescence maxima are also summarized in Table 1. Again the phosphorescence maxima of porphyrins (822-823 nm) are not affected by the fluorinated substituents. The triplet excited states of the porphyrins were detected from the transient absorption spectra measured 4.0 ns after laser excitation at 355 nm. A typical example is shown in Figure 4 for the case of **3**. The negative absorption at 410 nm in Figure 3 is due to bleaching of the ground-state absorption

Figure 4

bands. The positive absorption at 450 nm in Figure 4 is due to the triplet-triplet (T-T) transition. The T-T absorption decay obeys first-order kinetics as shown in Figure 5. This indicates that there is no contribution of the triplet-triplet annihilation under the present experimental conditions.

Figure 5

The T-T absorption maxima and the triplet lifetimes are summarized in Table 2. The triplet

lifetimes of porphyrins are in the range of 8.3–25 μs , which are shorter than the lifetimes of chlorin **30** (185 μs) and the bacteriochlorin **31** (77 μs).

Table 2

The decay of the T-T absorption in oxygen-saturated PhCN is enhanced significantly over what is observed in deaerated PhCN. The decay rate obeys first-order kinetics and the decay rate constant increases with increasing oxygen concentration. Thus, an efficient energy transfer from the triplet excited state of **3** to oxygen occurs to produce singlet oxygen. The rate constants of the energy transfer (k_{EN}) were determined from the dependence of the decay rate constants on oxygen concentration as listed in Table 2. The k_{EN} values are in the range of $8.9 \times 10^8 - 1.1 \times 10^9 \text{ M}^{-1} \text{ s}^{-1}$. There is no specific effects of the fluorinated substituents on the k_{EN} values which are smaller than the diffusion-limited value in PhCN ($5.6 \times 10^9 \text{ M}^{-1} \text{ s}^{-1}$).¹⁶

Irradiation of an oxygen-saturated benzene solution of **3** results in formation of singlet oxygen which was detected by the $^1\text{O}_2$ emission at 1270 nm (see Experimental Section). Quantum yields (Φ) of $^1\text{O}_2$ generation were determined from the emission intensity which was compared to the intensity obtained using a C_{60} reference compound.¹⁷ Relatively high Φ values are obtained for all investigated compounds as summarized in Table 2. The highest Φ value is obtained as 0.81 for the tetrafluorinated compound **3**.

Electrochemical studies. The electrochemically investigated compounds can be divided into three groups based on the macrocycle and substituents. The first group includes the four fluorinated porphyrins **1**, **2**, **3** and **4** (Chart 1, Scheme 2), the second, the four non-fluorinated porphyrins **26**, **27**, **28** and **29** (Scheme 2) and the third, the one fluorinated chlorin **30** and the one fluorinated bacteriochlorin **31** (Scheme 3). The electrochemistry of these ten complexes was

carried out in PhCN containing 0.1 M TBAP as supporting electrolyte. The half-wave or peak potential for each reduction is listed in Table 3.

In all but one case (compound **29**), the first reduction was reversible and the second irreversible due to a chemical reaction following formation of the dianion. This led to cyclic voltammograms of the type illustrated in Figure 6. A chemical reaction also followed the first oxidation of each porphyrin and this led to irreversible or quasi-reversible oxidations as graphically shown in Figure 7 for the case of compounds **3** and **4**. The UV-visible spectral changes obtained upon the first reduction were recorded in PhCN containing 0.2 M TBAP. An example of the thin-layer spectral changes is shown in Figure 8 for compounds **3** and **30** and a summary of the spectral data for the eight singly reduced porphyrins is given in Table 3. The neutral compounds have a Soret band at 407-412 nm and four visible bands between 503 and 626 nm (see Table 4). Upon the first reduction, the Soret and visible bands decrease in intensity while a new broad visible band appears at 799-813 nm (see Table 3). These results are consistent with a one-electron addition to the porphyrin π -ring system and indicate the formation of a porphyrin π -anion radical.¹⁸ The same spectral patterns are observed for the eight porphyrins in Table 3 and these data may be contrasted to what is observed for reduction of the chlorin **30** (Figure 8b) and bacteriochlorin **31** whose π -anion radical absorption bands are also summarized in this table. The spectral changes obtained upon oxidation of the porphyrin **3** and the chlorin **30** are illustrated in Figure 8. The reaction of the porphyrin is quasi-reversible while that of the chlorin is reversible on the cyclic voltammetry timescale (see cyclic voltammogram Figure 7). Thus only the spectrum of the chlorin **30** corresponds to a true measurement of the first electrogenerated oxidation product which should be a π -cation radical. The oxidations of other compounds were not chemically or electrochemically reversible (see Figure 7) and thus no meaningful spectra could

be obtained.

Figures 6-9, Table 3 and Table 4

***In vitro* Photosensitizing Efficacy.** The *in vitro* photosensitizing activity of fluorinated photosensitizers 1-4 was determined in radiation induced fibrosarcoma (RIF) tumor cell lines.¹⁹ For determining the drug dose, one of the fluorinated porphyrins 4 was initially tested at two different concentrations (0.5 and 1.0 μM). The drug concentration at 1.0 μM , together with a light dose at 4.0 J/cm², produced a significant phototoxicity without any dark toxicity. Other photosensitizers were then evaluated under similar drug concentration. From the results summarized in Figure 10 it can be seen that all the fluorinated porphyrins, the chlorin and the bacteriochlorin produced significant *in vitro* efficacy. However, the compounds in the porphyrin series containing bis-trifluoromethyl groups were found to be less effective than those containing tetrakis-trifluoromethyl groups. The *vic*-dihydroxy chlorin 30 and the related tetrahydroxy-bacteriochlorin 31 were quite effective with similar efficacy. In order to correlate the singlet oxygen efficiency with photosensitizing activity, these compounds were also evaluated for their photophysical characteristics. Although the presence and position of the fluorinated substituents in the porphyrin macrocycle produced a remarkable difference in singlet oxygen producing efficiency, no direct correlation was observed between singlet oxygen yield and *in vitro* photodynamic activity. For example, the singlet oxygen yields of porphyrins 1-3, are quite similar (0.61-0.81) but these compounds showed a significant difference in photosensitizing activity. In contrast, similar photosensitizing results were obtained among the tetrakis-trifluorinated analogs (3 and 4) in spite of a significant difference in singlet oxygen yields (0.81 and 0.36, respectively).

Figure 10

On the basis of *in vitro* results, it is difficult to predict the *in vivo* photosensitizing efficacy of these photosensitizers because the pharmacokinetic and pharmacodynamic profiles as well as photobleaching characteristics play important roles in drug localization and clearance. These properties could also be influenced by the overall lipophilicity of the molecule which has proven to be an important molecular descriptor that often is well correlated with the bioactivity of drugs. Lipophilicity is indicated by lipophilic indices such as the logarithm of a partition coefficient, log P, which reflects the equilibrium partitioning of a molecule between a nonpolar and a polar phase, such as n-octanol/water system. Partition coefficients can be measured either experimentally by following a simple "shake flask" approach or by using a currently available computer program (Pallas system). We calculated the log P values of the fluorinated porphyrins 1-4, the chlorin 30 and the bacteriochlorin 31 and these were in the range of 15.58-19.75 [1 and 2: 15.58, 3: 19.75 and 4: 18.43]. For investigating a correlation between singlet oxygen yields and PDT efficacy, the *in vivo* studies of fluorinated photosensitizers at different drug/light doses are currently in progress. These results along with the *in vivo* ^{19}F tumor imaging data will be reported elsewhere.

Intracellular Localization: In general, porphyrin-based compounds have shown very diverse patterns of localization, based on structure, lipophilicity and charge.²⁰ Localization in the lysosomes and mitochondria are reported to be predominant. However, in a QSAR study of certain photosensitizers the compounds that localize in mitochondria are generally found to be more effective. Therefore, the site of localization of the fluorinated porphyrin 4 and the related chlorin 30 and bacteriochlorin 31 were compared with Rhodamine-123 which is known to target mitochondria. Images of the photosensitizers and Rhodamine-123 were taken in rapid succession. The images result clearly indicate that these photosensitizers localize to the same

cellular region as Rhodamine-123, suggesting that these compounds localize in mitochondria, a more sensitive site for cell damage by PDT (see Figure 11 for a representative example).

Figure 11

Experimental

Chemistry. All chemicals were of reagent grade and used as received. Solvents were dried using standard methods unless stated otherwise. Reactions were carried out under a N₂ atmosphere and were monitored by analytical precoated (0.20 mm) silica TLC plates (POLYGRAM[®] SIL N-HR). Melting points were determined on electrically heated melting point apparatus and are uncorrected. UV-vis spectra were recorded on a Varian (Cary-50 Bio) spectrophotometer. ¹H and ¹⁹F-NMR spectra were recorded on a Bruker AMX 400 and 376.5 MHz NMR spectrometer respectively at 303 °K in CDCl₃ containing tetramethylsilane (TMS) as an internal standard. Proton chemical shifts (δ) are reported in parts per million (ppm) relative to TMS (0.00 ppm) or CDCl₃ (7.26 ppm) while fluorine chemical shifts are reported in ppm relative to trifluoroacetic acid (0.00 ppm). Coupling constants (*J*) are reported in Hertz (Hz) and s, d, t, q, m, dd and br refer to singlet, doublet, triplet, quartet, multiplet, doublet of doublet and broad respectively. Mass spectral data were obtained from the University of Michigan, East Lansing, MI and from the Biopolymer Facility of Basic Studies Center, Roswell Park Cancer Institute, Buffalo, NY. Elemental analysis data were obtained from Midwest Microlab, LLC, Indianapolis, IN.

General method for the synthesis of dipyrromethane 6, 7 and 8. Pyrrole 5 (10.0 g, 0.055 mol) and *p*-methoxy benzaldehyde (3.74 g, 0.0275 mol) were dissolved in ethanol (70 mL) and *p*-toluenesulfonic acid (200 mg) was added. The reaction mixture was refluxed for 2 hours under nitrogen. Analytical TLC at frequent intervals was used to monitor the completion of the

reaction. It was then cooled, the solid was filtered, the product was washed with cold water and dried under vacuum at room temperature. The desired pyrromethane **6** [3,9-diethyl-6-(*p*-methoxyphenyl)-4,8-dimethyl-2,10-diethoxycarbonyl dipyrromethane] was isolated as a white powder in 80% (21.2 g) yield.

3,9-diethyl-6-(*p*-methoxyphenyl)-4,8-dimethyl-2,10-diethoxycarbonyl dipyrromethane (6).

Mp 105-108 °C; ¹H NMR: δ 8.20 (brs, 2H, 2 X NH), 7.01 (d, *J* = 8.9, 2H, ArH), 6.87 (d, *J* = 8.9, 2H, ArH), 5.43(s, 1H, CH), 4.26 (q, *J* = 7.3, 4H, 2 x OCH₂CH₃), 3.81 (s, 3H, OCH₃), 2.74(q, *J* = 7.5, 4H, 2 X CH₂CH₃), 1.78 (s, 6H, 2 X CH₃), 1.31 (t, *J* = 7.1, 6H, 2 X OCH₂CH₃), 1.12 (t, *J* = 7.7, 6H, 2 X CH₂CH₃). Anal. Calcd for C₂₈H₃₆N₂O₄: C, 69.98; H, 7.55; N, 5.83. Found: C, 70.15; H, 7.37; N, 5.93. By following a similar approach, pyrrole **5** was reacted with *m*-methoxy or 3,5-dimethoxy benzaldehyde and the corresponding dipyrromethane **7** and **8** were synthesized.

3,9-Diethyl-6-(*m*-methoxyphenyl)-4,8-dimethyl-2,10-diethoxycarbonyl dipyrromethane (7).

Yield 70%; mp 122-125 °C ; ¹H NMR : δ 8.25 (brs, 2H, 2 x NH), 7.23-7.27 (m, 1H, ArH), 6.82 (dd, *J* = 2.2, 7.8, 1H, ArH), 6.68 (d, *J* = 7.4, 1H, ArH), 6.63 (s, 1H, ArH), 5.45 (s, 1H, CH), 4.25 (q, *J* = 7.3, 4H, 2 X OCH₂CH₃), 3.76 (s, 3H, OCH₃), 2.73 (q, *J* = 7.6, 4H, 2 X CH₂CH₃), 1.79 (s, 6H, 2 X CH₃), 1.30 (t, *J* = 7.1, 6H, 2 X OCH₂CH₃), 1.11 (t, *J* = 7.3, 6H, 2 X CH₂CH₃). Anal. Calcd for C₂₈H₃₆N₂O₅: C, 69.98; H, 7.55; N, 5.83. Found: C, 70.08; H, 7.60; N, 5.82.

3,9-Diethyl-6-(3'5'-dimethoxyphenyl)4,8-dimethyl-2,10-diethoxycarbonyldipyrromethane

(8). Yield 60%; viscous oil; ¹H NMR : δ 8.25 (brs, 2H, 2 X NH), 6.38 (s, 1H, ArH), 6.24 (s, 2H, ArH), 5.39 (s, 1H, CH), 4.26 (q, *J* = 7.3, 4H, 2 X OCH₂CH₃), 3.74 (s, 6H, 2 X OCH₃), 2.70 – 2.78 (m, 4H, 2 X CH₂CH₃), 1.79 (s, 6H, 2 X CH₃), 1.32 (t, *J* = 7.2, 6H, 2 X OCH₂CH₃), 1.10 – 1.16 (m, 6H, 2 X CH₂CH₃).

General method for the preparation of pyrromethanes 9, 11, 13. The diethoxycarbonyl dipyrromethanes 6, 7 or 8 (for example 11.6 g of 6) were individually dissolved in ethylene glycol (250 mL). Sodium hydroxide (12 g, crushed powder) was added, and the reaction mixture was refluxed for 1 h. It was then cooled, diluted with dichloromethane (250 mL) and washed with water (2 X 200 mL). The dichloromethane layer was dried over anhydrous sodium sulfate. The residue obtained after evaporating the solvent was chromatographed over silica column eluted with chloroform. The appropriate eluates were combined, the solvent was evaporated, and the desired dipyrromethane 9 was obtained in 95% yield.

3,9-Diethyl-6-(*p*-methoxyphenyl)-4,8-dimethyl-dipyrromethane (9). Mp 64-66 °C ; lit.²¹ ¹H NMR : δ 7.30 (brs, 2H, 2 X NH), 7.06 (d, J = 8.8, 2H, ArH), 6.85 (d, J = 8.8, 2H, ArH), 6.38 (s, 2H, 2 X Pyrrolic CH), 5.45 (s, 1H, CH), 3.81 (s, 3H, OCH₃), 2.44 (q, J = 7.2, 4H, 2 X CH₂CH₃), 1.81 (s, 6H, 2 X CH₃), 1.19 (t, J = 7.9, 6H, 2 X CH₂CH₃).

3,9-Diethyl-6-(*m*-methoxyphenyl)-4,8-dimethyl-dipyrromethane (11). Yield 88%; mp 202-204 °C; ¹H NMR: δ 9.49 (s, 2H, 2 X CHO), 9.08 (brs, 2H, 2 X NH), 7.23-7.27 (m, 1H, ArH), 6.83 (dd, J = 2.5, 8.0, 1H, ArH), 6.66 (d, J = 7.6, 1H, ArH), 6.62 (s, 1H, ArH), 5.53 (s, 1H, CH), 3.75 (s, 3H, OCH₃), 2.71 (q, J = 7.6, 4H, 2 X CH₂CH₃), 1.86 (s, 6H, 2 X CH₃), 1.20 (t, J = 7.8, 6H, 2 X CH₂CH₃). Anal. Calcd for C₂₂H₂₈N₂O₂·2H₂O: C, 70.94; H, 8.66; N, 7.52. Found: C, 71.29; H, 7.17; N, 7.24.

3,9-Diethyl-6-(3',5'-dimethoxyphenyl)-4,8-dimethyl-dipyrromethane (13). Yield 97%; mp 119-121 °C ; ¹H NMR : δ 7.34 (brs, 2H, 2 X NH), 6.33-6.36 (m, 3H, ArH), 6.31 (s, 2H, 2 X Pyrrolic CH), 5.40 (s, 1H, CH), 3.74 (s, 6H, 2 X OCH₃), 2.40-2.45 (m, 4H, 2 X CH₂CH₃), 1.81 (s, 6H, 2 X CH₃), 1.14-1.19 (m, 6H, 2 X CH₂CH₃). Anal. Calcd for C₂₃H₃₀N₂O₂·5H₂O: C, 60.50; H, 8.83; N, 6.40. Found: C, 60.00; H, 8.82; N, 5.91.

General method for the preparation of diformyldipyrromethanes 10, 12 and 14. The pyrromethane(s) [e. g. 9 (7.1 g)] was dissolved in Vilsmeier reagent, prepared by reaction POCl_3 (10.5 mL) and DMF (45 mL) was added and the reaction mixture was stirred at room temperature overnight. The reaction mixture was poured into ice cold water (250 ml) and aqueous sodium hydroxide (50%, 35 mL) was then added slowly ; the pH was adjusted to 10-12 and stirred overnight before extracting with dichloromethane (3 X 200 mL). The organic layer was separated, washed with water (2 x 200 mL) until neutral and dried over anhydrous sodium sulfate. Evaporation of the solvent gave a residue which was chromatographed over a silica column, eluting with 1:1 ethyl acetate/cyclohexane. The major band was separated, and the product obtained after evaporating the solvent was crystallized with methanol and compound 10 was isolated in 80% (6.80 g) yield.

3,9-Diethyl-2,10-diformyl-6-(*p*-methoxyphenyl)-4,8-dimethyl-dipyrromethane (10). Mp 168-169 °C; ^1H NMR: δ 9.50 (s, 2H, 2 X CHO), 8.70 (brs, 2H, 2 X NH), 6.98(d, $J = 8.7$, 2H, ArH), 6.86 (d, $J = 8.7$, 2H, ArH), 5.47 (s, 1H, CH), 3.80 (s, 3H, OCH_3), 2.70 (q, $J = 7.5$, 4H, 2 X CH_2CH_3), 1.81 (s, 6H, 2 X CH_3), 1.20 (t, $J = 7.5$, 6H, 2 X CH_2CH_3). Anal. Calcd. for $\text{C}_{24}\text{H}_{28}\text{N}_2\text{O}_3 \cdot 1/2 \text{H}_2\text{O}$: C, 71.80; H, 7.28; N, 6.98. Found: C, 71.69; H, 6.74; N, 6.76.

3,9-Diethyl-2,10-diformyl-6-(*m*-methoxyphenyl)-4,8-dimethyl-dipyrromethane (12). Yield 79 %; mp 202-204 °C; ^1H NMR: δ 9.49 (s, 2H, 2 X CHO), 9.08 (brs, 2H, 2 X NH), 7.23-7.27 (m, 1H, ArH), 6.83 (dd, $J = 2.5, 8.0$, 1H, ArH), 6.66 (d, $J = 7.6$, 1H, ArH), 6.62 (s, 1H, ArH), 5.53 (s, 1H, CH), 3.75 (s, 3H, OCH_3), 2.71 (q, $J = 7.6$, 4H, 2 X CH_2CH_3), 1.86 (s, 6H, 2 X CH_3), 1.20 (t, $J = 7.8$, 6H, 2 X CH_2CH_3). Anal. Calcd for $\text{C}_{24}\text{H}_{28}\text{N}_2\text{O}_3$: C, 73.44; H, 7.19; N, 7.14. Found: C, 73.65; H, 7.29; N, 7.06.

3,9-Diethyl-2,10-diformyl-6-(3,5-di-methoxyphenyl)-4,8-dimethyl-dipyrromethane (14).

Yield 78%; mp 202-204 °C; ^1H NMR (CDCl_3 , 400 MHz) δ 9.52 (s, 2H, 2 x CHO), 8.56 (brs, 2H, 2 x NH), 6.40 (s, 1H, ArH), 6.20 (s, 2H, ArH), 5.42 (s, 1H, CH), 3.74 (s, 6H, 2 x OCH_3), 2.70 (q, $J = 7.7$, 4H, 2 x CH_2CH_3), 1.81 (s, 6H, 2 x CH_3), 1.20 (t, $J = 7.8$, 6H, 2 x CH_2CH_3). Anal. Calcd for $\text{C}_{25}\text{H}_{30}\text{N}_2\text{O}_4 \cdot 1/2\text{H}_2\text{O}$: C, 69.58; H, 7.24; N, 6.49. Found: 69.52; H, 7.00; N, 6.16.

General method for the Synthesis of porphyrins 22-25. The diformyl dipyrromethane (e. g. **10**, 2.52 g, 6.43 mmol), and dipyrromethane **18** (2.04 g, 6.42 mmol) were dissolved in dichloromethane (500 mL). *p*-Toluenesulfonic acid (6.0 g) dissolved in methanol (100 mL) was added, and the reaction mixture was stirred at room temperature overnight under nitrogen atmosphere. A saturated solution of zinc acetate/methanol (125 mL) was added, and the reaction was stirred for another 12 hours. It was then diluted with dichloromethane, washed with water and the organic layer was dried over anhydrous sodium sulfate. Evaporation of the solvent gave a residue which was dissolved in trifluoroacetic acid (30 mL) and stirred at room temperature for 30 min. The Zn-free porphyrin thus obtained after standard work-up was chromatographed over a short Grade III Alumina column and eluted with dichloromethane. The major band was collected and the solvent evaporated. The residue was crystallized from dichloromethane/hexane and porphyrin **22** was isolated in 17% (640 mg) yield.

2,8,13,17-Tetraethyl-5-(*p*-methoxyphenyl)-3,7,12,18-tetramethylporphyrin (22). Mp 280-282 °C; UV-vis [CH_2Cl_2 , nm (ϵ , $\text{M}^{-1}\text{cm}^{-1}$)] 403 (3.82×10^5), 503 (3.15×10^4), 535 (1.39×10^4), 571 (1.35×10^4), 623 (4.82×10^3); ^1H NMR : δ 10.13 (s, 2H, 2 X mesoH), 9.92 (s, 1H, mesoH), 7.86 (d, $J = 9.0$, 2H, ArH), 7.16 (d, $J = 9.0$, 2H, ArH), 4.00–4.06 (m, 8H, 4 X CH_2CH_3), 3.99 (s, 3H, OCH_3), 3.62 (s, 6H, 2 X CH_3), 2.47 (s, 6H, 2 X CH_3), 1.87 (t, $J = 7.7$, 6H, 2 X CH_2CH_3), 1.75 (t, $J = 7.6$, 6H, 2 X CH_2CH_3), -3.19 (brs, 1H, NH), -3.27 (brs, 1H, NH). Anal. Calcd for

$C_{39}H_{44}N_4O$: C, 80.10; H, 7.58; N, 9.58. Found: C, 80.14; H, 7.54; N, 9.62.

2,8,13,17-Tetraethyl-5-(*m*-methoxyphenyl)-3,7,12,18-tetramethylporphyrin (23). Yield 30%; mp 270-272 °C; 1H NMR: δ 10.16 (s, 2H, 2 X mesoH), 9.96 (s, 1H, meso H), 7.67 (d, J = 7.2, 2H, ArH), 7.59 (t, J = 7.8, 1H, ArH), 7.50 (s, 1H, ArH), 4.02–4.10 (m, 8H, 4 X CH_2CH_3), 4.00 (s, 3H, OCH_3), 3.65 (s, 6H, 2 X CH_3), 2.60 (s, 6H, 2 X CH_3), 1.90 (t, J = 7.7, 6H, 2 X CH_2CH_3), 1.78 (t, J = 7.94, 6H, 2 X CH_2CH_3), -3.20 (brs, 1H, NH), -3.35 (brs, 1H, NH). Anal. Calcd for $C_{39}H_{44}N_4O$: C, 80.10; H, 7.58; N, 9.58; Found: C, 80.76; H, 7.60; N, 9.54.

2,8-Diethyl-5-(3',5'-dimethoxyphenyl)-2,8-diethyl-13,17-bis-(2-methoxycarbonylethyl)-3,7,12,18-tetramethylporphyrin (25). The title compound was prepared by reacting diformyldipyrromethane **14** with dipyrromethane dicarboxylic acid **21** by following the procedure reported by Chen et al.²²

General method for the synthesis of porphyrins 26-29. Porphyrin **26-29** (100 mg) were obtained in 70-77% yield by reacting porphyrins **22-25** with etherial boron tribromide solution.

2,8,13,17-Tetraethyl-5-(*p*-hydroxyphenyl)-3,7,12,18-tetramethylporphyrin (26). Yield 77%; mp > 300 °C; UV-vis [CH_2Cl_2 , nm (ϵ , $M^{-1}cm^{-1}$)] 404 (3.79×10^5), 503 (2.91×10^4), 536 (1.19×10^4), 570 (1.14×10^4); 1H NMR : δ 10.15 (s, 2H, 2 X meso H), 9.94 (s, 1H, meso H), 7.89 (d, J = 9.2, 2H, ArH), 7.18 (d, J = 8.7, 2H, ArH), 4.00–4.08 (m, 8H, 4 X CH_2CH_3), 3.64 (s, 6H, 2 X CH_3), 2.53 (s, 6H, 2 X CH_3), 1.88 (t, J = 7.7, 6H, 2 X CH_2CH_3), 1.76 (t, J = 7.5, 6H, 2 X CH_2CH_3), -3.75 (brs, 2H, 2 x NH). Anal. Calcd for $C_{38}H_{42}N_4O$: C, 79.66; H, 7.42; N, 9.82; Found: C, 79.75; H, 7.45; N, 9.70.

2,8,13,17-Tetraethyl-5-(*m*-hydroxyphenyl)-3,7,12,18-tetramethylporphyrin (27). Yield 72%; mp > 300 °C; UV-vis [CH_2Cl_2 , nm (ϵ , $M^{-1}cm^{-1}$)] 402 (5.00×10^5), 502 (4.03×10^4), 536 (1.76×10^4), 570 (1.61×10^4), 623 (4.60×10^3); 1H NMR : δ 10.18 (s, 2H, 2 x meso H), 9.98 (s,

1H, mesoH), 7.69 (d, $J = 7.0$, 2H, ArH), 7.61 (t, $J = 7.7$, 1H, ArH), 7.51 (s, 1H, ArH), 4.04 – 4.12 (m, 8H, 4 X CH_2CH_3), 3.66 (s, 6H, 2 X CH_3), 2.58 (s, 6H, 2 X CH_3), 1.91 (t, $J = 7.7$, 6H, 2 X CH_2CH_3), 1.79 (t, $J = 7.94$, 6H, 2 X CH_2CH_3), -3.85 to -3.75 (each brs, 1H, 2 X NH); Anal. Calcd for $\text{C}_{38}\text{H}_{42}\text{N}_4\text{O}$: C, 79.66; H, 7.42; N, 9.82. Found: C, 80.02; H, 7.37; N, 9.83.

2,8,13,17-Tetraethyl-5-(3',5'-di-hydroxyphenyl)-3,7,12,18-tetramethylporphyrin (28).

Yield 75 %; mp > 300 °C; UV-vis [CH_2Cl_2 , nm (ϵ , $\text{M}^{-1}\text{cm}^{-1}$)] 402 (4.16×10^5), 502 (3.45×10^4), 536 (1.62×10^4), 569 (1.49×10^4), 623 (6.50×10^3); ^1H NMR (CDCl_3 , 400 MHz) δ 10.18 (s, 2H, 2 X mesoH), 9.98 (s, 1H, meso H), 7.05 (s, 2H, ArH), 6.69 (s, 1H, ArH), 4.04– 4.12 (m, 8H, 4 X CH_2CH_3), 3.66 (s, 6H, 2 X CH_3), 2.67 (s, 6H, 2 X CH_3), 1.90 (t, $J = 7.7$, 6H, 2 X CH_2CH_3), 1.80 (t, $J = 7.5$, 6H, 2 X CH_2CH_3). Anal. Calcd for $\text{C}_{38}\text{H}_{42}\text{N}_4\text{O}_2 \cdot \text{H}_2\text{O}$: C, 75.47; H, 7.33; N, 9.26. Found: C, 75.31; H, 7.38; N, 9.14.

2,8-Diethyl-5-(3',5'-dimethoxyphenyl)-13,17-bis-(2-methoxycarbonylethyl)-3,7,12,18-

tetramethylporphyrin (29). Yield 70%; mp > 300 °C; UV-vis [CH_2Cl_2 , nm (ϵ , $\text{M}^{-1}\text{cm}^{-1}$)] 403 (4.64×10^5), 502 (5.21×10^4), 536 (3.39×10^4), 571 (4.00×10^4); ^1H NMR : δ 10.18 (s, 2H, 2 X mesoH), 9.95 (s, 1H, mesoH), 7.10 (s, 2H, ArH), 6.70 (s, 1H, ArH), 4.30– 4.40 (m, 4H, 2 X $\text{CH}_2\text{CH}_2\text{CO}_2\text{CH}_3$), 3.98–4.08 (m, 4H, 2 X CH_2CH_3), 3.70 (s, 6H, 2 X OCH_3), 3.65 (s, 6H, 2 X CH_3), 3.30–3.40 (m, 4H, 2 X $\text{CH}_2\text{CH}_2\text{CO}_2\text{CH}_3$), 2.66 (s, 6H, 2 X CH_3), 1.80– 1.90 (m, 6H, 2 X CH_2CH_3). Anal. Calcd for $\text{C}_{42}\text{H}_{46}\text{N}_4\text{O}_6 \cdot \text{H}_2\text{O}$: C, 63.69; H, 6.11; N, 7.08. Found: C, 63.32; H, 6.07; N, 6.41.

General method for the synthesis of porphyrins 1 to 4. 3,5-Bis(trifluoromethyl)benzylbromide (40 μL , 0.22 mmol) and anhydrous K_2CO_3 (250 mg) were added to a stirred solution of 5-(4-hydroxyphenyl)tetraethylporphyrin **26** (85 mg, 0.15 mmol) in dry acetonitrile (10 mL) and the reaction mixture was refluxed overnight under nitrogen. Solvent was evaporated under reduced

pressure; water (20 mL) was poured and extracted with CH_2Cl_2 (2 x 20 mL). The combined organic extracts were washed with water (2 X 20 mL) and organic fraction was dried over Na_2SO_4 . Removal of organic solvent *in vacuo* gave a crude solid residue, which was chromatographed over silica column using CH_2Cl_2 as an eluant to yield 77 mg (65%) of 5-[4-{3,5-Bis(trifluoromethyl)benzyloxy}phenyl]tetraethylporphyrin **1** as purple plates.

5-[4-{3,5-Bis(trifluoromethyl)benzyloxy}phenyl]-2,8,13,17-tetraethyl-3,7,12,18-tetramethyl porphyrin (1). Mp. 274-276 °C; UV-vis [CH_2Cl_2 , nm (ϵ , $\text{M}^{-1}\text{cm}^{-1}$)] 403 (2.52×10^5), 502 (2.08×10^4), 535 (9.25×10^3), 570 (8.82×10^3), 624 (3.13×10^3); ^1H NMR: δ 10.21 (s, 2H, 2 X meso CH), 10.00 (s, 1H, meso CH), 8.14 (s, 2H, ArH), 7.98 (s, 1H, ArH), 7.96 (d, $J=4.5$, 2H, ArH), 7.31 (d, $J=4.5$, 2H, ArH), 5.42 (s, 2H, OCH_2), 4.06-4.13 (m, 8H, 4X X CH_2CH_3), 3.70 (s, 6H, 2 X CH_3), 2.52 (s, 6H, 2 X CH_3), 1.94 (t, $J=7.7$, 6H, 2 X CH_2CH_3), 1.82 (t, $J=7.5$, 6H, 2 X CH_2CH_3). ^{19}F NMR: δ 13.12 (s, 6F, 2 X CF_3). Anal. Calcd for $\text{C}_{47}\text{H}_{46}\text{N}_4\text{F}_6\text{O} \cdot \text{H}_2\text{O}$: C, 69.27; H, 5.94; N, 6.87. Found: C, 69.37; H, 6.19; N, 6.33.

5-[3-Bis{3,5-trifluoromethyl}benzyloxy}phenyl]-2,8,13,17-tetraethyl-3,7,12,18-tetramethyl porphyrin (2). Yield 96%; mp 109-110 °C; UV-vis [CH_2Cl_2 , nm (ϵ , $\text{M}^{-1}\text{cm}^{-1}$)] 404 (9.49×10^4), 501 (6.83×10^3), 537 (4.27×10^3), 570 (4.98×10^3); ^1H NMR : δ 10.17 (s, 2H, 2 X meso CH), 9.96 (s, 1H, meso CH), 7.94 (s, 2H, ArH), 7.75-7.85 (m, 3H, ArH), 7.62 (t, $J=7.8$, 1H, ArH), 7.40 (dd, $J=2.6$ and 7.8, 1H, ArH), 5.32 (s, 2H, OCH_2), 4.00-4.10 (m, 8H, 4 X CH_2CH_3), 3.65 (s, 6H, 2 X CH_3), 2.53 (s, 6H, 2 X CH_3), 1.89 (t, $J=7.8$, 6H, 2 X CH_2CH_3), 1.77 (t, $J=7.6$, 6H, 2 X CH_2CH_3), -3.10 and -3.30 (each brs, 1H, 2 X NH). ^{19}F NMR: δ 13.00 (s, 6F, 2 x CF_3). Anal. Calcd for $\text{C}_{47}\text{H}_{46}\text{N}_4\text{F}_6\text{O} \cdot \text{Na}_2\text{SO}_4$: C, 60.12; H, 4.94; N, 5.96. Found: C 62.40, H 4.85, N 5.26.

5-[3',5'-Bis{3'',5''-trifluoromethyl}benzyloxy}phenyl]-2,8,13,17-tetraethyl-3,7,12,18-tetramethyl porphyrin (3). Yield 45%; mp 214-216 °C; UV-vis[CH₂Cl₂, nm (ε, M⁻¹cm⁻¹)] 403 (2.29 X 10⁵), 502 (1.93 X 10⁴), 536 (9.27 X 10³), 570 (8.53 X 10³), 623 (3.34 X 10³); ¹H NMR: δ 10.20 (s, 2H, 2 X meso CH), 9.98 (s, 1H, meso CH), 7.96 (s, 4H, ArH), 7.87 (s, 2H, ArH), 7.42 (d, *J*=2.9, 2H, ArH), 7.12-7.16 (m, 1H, ArH), 5.37 (s, 4H, 2 x OCH₂), 4.03-4.10 (m, 8H, 4 X CH₂CH₃), 3.66 (s, 6H, 2 X CH₃), 2.60 (s, 6H, 2 X CH₃), 1.91 (t, *J*=7.5, 6H, 2 X CH₂CH₃), 1.78 (t, *J*=7.5, 6H, 2 X CH₂CH₃). ¹⁹F NMR: δ 12.98 (s, 12F, 4 X CF₃). Anal. Calcd for C₅₆H₅₀N₄F₁₂O₂: C, 64.74; H, 4.85; N, 5.39. Found: C, 64.20; H, 4.94; N, 5.00.

5-[3',5'-Bis{3'',5''-trifluoromethyl}benzyloxy}phenyl]-2,8-diethyl-13,17-bis(2-methoxycarbonylethyl)-3,7-dimethylporphyrin (4). Yield 75%; mp 72-75 °C; UV-vis [CH₂Cl₂, nm (ε, M⁻¹cm⁻¹)] 404 (3.81 X 10⁵), 502 (3.02 X 10⁴), 536 (1.41 X 10⁴), 570 (1.32 X 10⁴), 624 (4.82 X 10³), 653 (2.59 X 10³); ¹H NMR : δ 10.16 (s, 2H, 2 X meso CH), 9.97 (s, 1H, meso CH), 7.92 (s, 3H, ArH), 7.81-7.84 (m, 3H, ArH), 7.37 (d, *J*=2.0, 2H, ArH), 7.11 (d, *J*=2.4, 1H, ArH), 5.35 (s, 4H, 2 X OCH₂), 4.40 (t, *J*=7.6, 4H, 2 X CH₂CH₂CO₂CH₃), 4.00 (q, *J*=7.8, 4H, 2 X CH₂CH₃), 3.67 (s, 6H, 2 X OCH₃), 3.66 (s, 6H, 2 X CH₃), 3.30 (t, *J*=7.6, 4H, 2 X CH₂CH₂CO₂CH₃), 2.56 (s, 6H, 2 X CH₃), 1.74 (t, *J*=7.4, 6H, 2 X CH₂CH₃), -3.27 (brs, 1H, NH), -3.33 (brs, 1H, NH). ¹⁹F NMR : δ 12.96 (s, 12F, 4 X CF₃). Anal. Calcd for C₆₀H₅₄N₄F₁₂O₆: C, 62.39; H, 4.71; N, 4.85. Found: C, 61.56; H, 4.71; N, 4.71.

5-{3',5'-Bis(3'',5''-dimethylbenzyloxy)}phenyl-2,8-diethyl-13,17-bis(2-methoxycarbonyl ethyl) -3,7-dimethylporphyrin (4a): Yield 30%; mp 158-160 °C; UV-vis [CH₂Cl₂, nm (ε, M⁻¹cm⁻¹)] 404 (3.81 X 10⁵), 502 (3.43 X 10⁴), 536 (1.56 X 10⁴), 570 (1.50 X 10⁴), 623 (5.19 X 10³); ¹H NMR (CDCl₃, 400 MHz) δ 10.18 (s, 2H, 2 X meso CH), 9.98 (s, 1H, meso CH), 7.31-7.32 (m, 2H, ArH), 7.11 (brs, 1H, ArH), 7.08 (s, 3H, ArH), 6.99 (s, 1H, ArH), 6.96 (brs, 2H, ArH),

5.17 (s, 4H, 2 X OCH₂), 4.42 (t, $J=7.6$, 4H, 2 X CH₂CH₂CO₂CH₃), 4.04 (q, $J=7.0$, 4H, 2 X CH₂CH₃), 3.70 (s, 6H, 2 X OCH₃), 3.69 (s, 6H, 2 X CH₃), 3.32 (t, $J=7.8$, 4H, 2 X CH₂CH₂CO₂CH₃), 2.58 (s, 6H, 2 X CH₃), 2.30 (s, 12H, 4 X PhCH₃), 1.78 (t, $J=7.4$, 6H, 2 X CH₂CH₃), -3.25 (brs, 1H, NH), -3.28 (brs, 1H, NH). Mass Calcd for C₆₀H₆₆N₄O₆: 939.22. Found: 939.20

Synthesis of chlorin 30 and bacteriochlorin 31 from porphyrin 4. OsO₄ (75 mg) dissolved in diethyl ether (5 mL) was added to a stirred solution of **4** (100 mg) in dry CH₂Cl₂ (20 mL) and pyridine (0.2 mL). The reaction mixture was stirred at room temperature for 6 hrs. UV-vis spectrum showed two peaks at 645 nm (chlorin **30**, major, $R_f = 0.6$ in 5% MeOH in CH₂Cl₂) and at 713 nm (bacteriochlorin **31**, minor, $R_f = 0.4$ in 5% MeOH in CH₂Cl₂). The reaction was worked up by passing a stream of H₂S gas for one minute, diluted with CH₂Cl₂ (50 mL) and then filtered through fluted filter paper. The residue was washed with CH₂Cl₂ (3 X 50 mL), dried over Na₂SO₄. The solvent was concentrated and the crude mixture so obtained was purified by preparative TLC using 5% MeOH in CH₂Cl₂ as an eluant. Three bands were isolated. The fast moving band (10 mg) was identified as unreacted starting material **4**, the middle band (25 mg, 40%) was found to be chlorin **30** and the slowest moving band isolated in 13 mg (20%) was characterized as bacteriochlorin **31**.

5-[3,5-Bis{3,5-bis(trifluoromethyl)benzyloxy}phenyl]-2,8-diethyl-7,8-dihydroxy-3,7,12,18-tetramethyl-13,17-bis(2-methoxycarbonylethyl)porphyrin (30). Mp 172-174 °C; UV-vis [CH₂Cl₂, nm (ϵ , M⁻¹cm⁻¹)] 397 (4.44 X 10⁵), 500 (4.16 X 10⁴), 648 (1.17 X 10⁵); ¹H NMR: δ 9.88 (s, 1H, meso CH), 9.61 (s, 1H, meso CH), 9.21 (s, 1H, meso CH), 7.97 (s, 2H, ArH), 7.91 (s, 2H, ArH), 7.88 (s, 1H, ArH), 7.84 (s, 1H, ArH), 7.35 (s, 1H, ArH), 7.12 (s, 1H, ArH), 7.06 (s, 1H, ArH), 5.40 (s, 2H, OCH₂), 5.30 (s, 2H, OCH₂), 4.24 (t, $J=7.2$, 2H, CH₂CH₂CO₂CH₃), 4.15 (t,

$J=7.4$, 2H, $\text{CH}_2\text{CH}_2\text{CO}_2\text{CH}_3$), 3.96 (q, $J=7.4$, 2H, CH_2CH_3), 3.69 (s, 3H, OCH_3), 3.67 (s, 3H, OCH_3), 3.47 (s, 3H, CH_3), 3.44 (s, 3H, CH_3), 3.17 (t, $J=7.6$, 4H, 2 X $\text{CH}_2\text{CH}_2\text{CO}_2\text{CH}_3$), 2.26 (s, 3H, CH_3), 2.23-2.34 (m, 3H, CH_3), 1.70 (t, $J=7.8$, 3H, CH_3), 0.89-0.93 (m, 2H, CH_2CH_3), 0.44 (t, $J=8.0$, 3H, CH_2CH_3), -2.32 (brs, 1H, NH), ^{19}F NMR: δ 12.98 (s, 6F, 2 X CF_3), 12.99 (s, 6F, 2 X CF_3). Mass Calcd. for $\text{C}_{60}\text{H}_{56}\text{N}_4\text{F}_{12}\text{O}_8$: 1189.12. Found: 1189.50

5-[3,5-Bis{3,5-bis(trifluoromethyl)benzyloxy}phenyl]-2,8-diethyl-7,8,17,18-tetrahydroxy-3,7,12,18-tetramethyl-13,17-bis (2-methoxycarbonylethyl)porphyrin (31).

Mp 100-103 °C; UV-vis (CH_2Cl_2) 395 (1.69×10^5), 504 (2.22×10^4), 644 (3.81×10^4), 716 (2.67×10^4). Note : Due to mixture of isomers it was difficult to assign the resonances for each proton in the ^1H NMR spectrum. The ^{19}F NMR spectrum showed mainly two peaks at δ 12.97 and 12.96 ppm. Mass calcd for $\text{C}_{60}\text{H}_{58}\text{N}_4\text{F}_{12}\text{O}_{10}$: 1223.13. Found: 1223.30

Method for *in vitro* biological studies: The *in vitro* photosensitizing activity of fluorinated photosensitizers 1-4, chlorin 30 and bacteriochlorin 31 was determined in the radiation induced fibrosarcoma (RIF) tumor cell line.¹⁸ The RIF tumor cells were grown in α -MEM with 10% fetal calf serum, penicillin and streptomycin. Cells were maintained in 5% CO_2 , 95% air and 100% humidity. For determining the PDT efficacy, these cells were plated in 96-well plates at a density of 1.25×10^4 cells well in complete media. After an overnight incubation at 37°C, the photosensitizers were added at the same concentration (2.0 μM), incubated at 37 °C for 3 hrs in the dark, washed once with PBS. Cells were then illuminated with a 1000W quartz halogen lamp with IR and band pass dichroic filters to allow light between 400-700 nm, at a dose rate of 16 mW/cm^2 . After PDT, the cells were washed once and placed in complete media and incubated for 48 hours. Then 10 μL of 5.0mg/mL solution of 3-[4,5-dimethylthiazol-2-yl]-2,5-diphenyltetrazoliumbromide dissolved in PBS (Sigma, St. Louis, MO) was added to each well.

After a 4 hr incubation at 37 °C the MTT and media were removed and 100 μ L DMSO was added to solubilize the formazin crystals. The 96-well plate was read on a microtiter plate reader (Miles Inc. Titertek Multiscan Plus MK II) at 560 nm. The results were plotted as percent survival of the corresponding dark (drug no light) control for each compound tested. Each data point represents the mean from 3 separate experiments, and the error bars are the standard deviation. Each experiment was done with 5 replicate wells.

Intracellular Localization: In order to determine the subcellular localization of the fluorinated porphyrin **4**, chlorin **30** and bacteriochlorin **31**, the RIF cells were seeded on poly-L-lysine coated glass cover slips at 1×10^5 in 6 well plates and cultured for 48 hrs to allow for attachment and spreading. The cells were incubated at 37 °C in dark with the 1 μ M concentration of photosensitizers for 1h, 4 hrs and 24 hrs and then co-incubated with the 0.25 μ M concentration of the organelle-specific dyes Rhodamine-123 for mitochondria and Fluospheres for lysosomes. Immediately prior to microscopy (Zeiss Axiovert 35, Carl Zeiss, Inc. Germany), the cells were gently rinsed with PBS. Cells were illuminated with a mercury arc lamp with a filter cube containing 530-585 nm excitation filter, a 600 nm dichoric filter and a long pass emission filter to detect the photosensitizer. Fluorescent images were recorded and analyzed using a GenIISys intensifier coupled to a Dage MTI CCD72 camera and digitally processed with Metamorph software (Universal Imaging Corp., Downingtown, PA).

Photophysical Measurements. Absorption spectra were recorded on a Hewlett Packard 8453A diode array spectrophotometer. Time-resolved fluorescence and phosphorescence spectra were measured by a Photon Technology International GL-3300 with a Photon Technology International GL-302, nitrogen laser/pumped dye laser system, equipped with a four channel digital delay/pulse generator (Stanford Research System Inc. DG535) and a motor driver (Photon

Technology International MD-5020). Excitation wavelengths were from 535 to 551 nm using coumarin 540A (Photon Technology International, Canada) as a dye. Fluorescence lifetimes were determined by a two-exponential curve fit using a microcomputer. Nanosecond transient absorption measurements were carried out using a Nd:YAG laser (continuum, SLII-10, 4-6 ns fwhm) at 355 nm with the power of 10 mJ as an excitation source. Photoinduced events were estimated by using a continuous Xe-lamp (150 W) and an InGaAs-PIN photodiode (Hamamatsu 2949) as a probe light and a detector, respectively. The output from the photodiodes and a photomultiplier tube was recorded with a digitizing oscilloscope (Tektronix, TDS3032, 300 MHz). The transient spectra were recorded using fresh solutions in each laser excitation. All experiments were performed at 298 K.

For the $^1\text{O}_2$ phosphorescence measurements, an O_2 -saturated C_6D_6 solution containing the sample in a quartz cell (optical path length 10 mm) was excited at 532 nm using a Cosmo System LVU-200S spectrometer. A photomultiplier (Hamamatsu Photonics, R5509-72) was used to detect emission in the near infrared region (band path 1 mm).

Electrochemical and Spectroelectrochemical Measurements. Cyclic voltammetry (CV) measurements were performed at 298 K on an EG&G Model 173 potentiostat coupled with an EG&G Model 175 universal programmer in deaerated benzonitrile solution containing 0.10 M TBAP as a supporting electrolyte. A three-electrode system was utilized and consisted of a glassy carbon working electrode, a platinum wire counter electrode and a saturated calomel reference electrode (SCE). The reference electrode was separated from the bulk of the solution by a fritted-glass bridge filled with the solvent/supporting electrolyte mixture. Thin-layer spectroelectrochemical measurements of the one-electron oxidized and one-electron reduced bacteriochlorin derivatives were carried out using an optically transparent platinum thin-layer

working electrode and a Hewlett-Packard model 8453 diode array spectrophotometer coupled with an EG&G Model 173 universal programmer.

In vivo ^{19}F measurements. The Radiation induced fibrosarcoma (RIF) cells were maintained according to the protocol of Twentyman et al ²³. Tumors were grown on mouse foot dorsum by inoculating 2×10^5 cells. The three diameters of the foot tumor were measured using calipers and the volume calculated by an ellipsoid approximation. The tumor volumes were in the range of 150-250 mm³. The photosensitizer was administered IP ($\sim 100\mu\text{M/kg}$). ^{19}F MR spectra were collected on a Bruker 7T instrument using a home built surface coil. The ^{19}F MR spectral parameters consisted of a 16 μs pulse width, a spectral width of 20 KHz, 8K data points, and a 2s repetition time. The raw data was apodized with 50-100 Hz exponential line broadening before Fourier transformation.

Acknowledgments

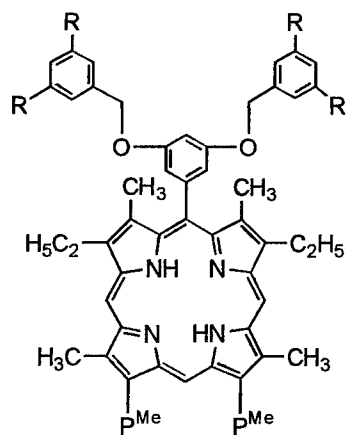
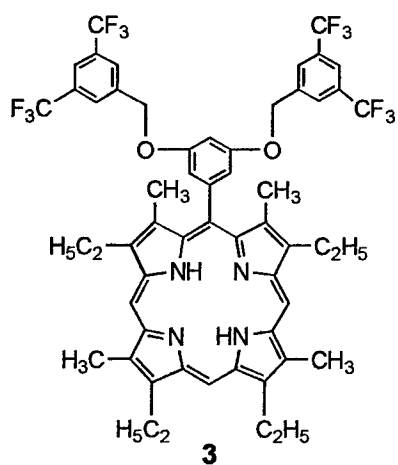
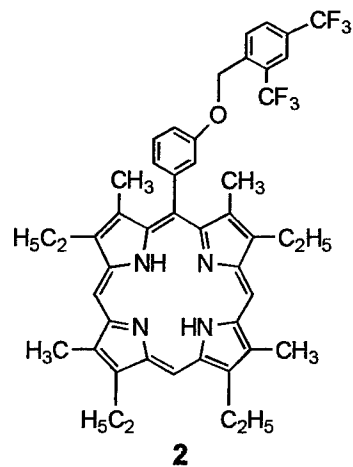
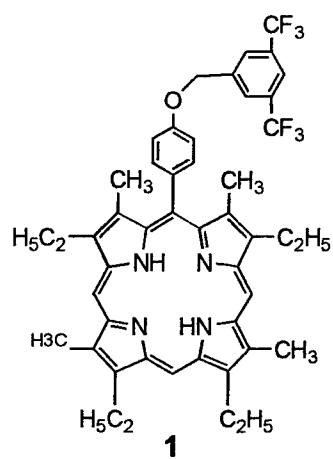
This research was supported by grants from DOD (DMAD17-99-1-9065), NIH (CA 55792), the Robert A. Welch Foundation (Grant E-680 to KMK), from the Ministry of Education, Culture, Sports, Science and Technology, Japan (13440216 and 13031059 to SF) and the shared resources of the Roswell Park Cancer Center Support Grant (P30CA16056). We thank Beverly Chamberlin, Michigan State University, East Lansing for mass spectrometry results. The elemental analyses were performed at Midwest Micro lab, Indianapolis.

References.

1. (a) Pandey, R. K. and Zheng, G. in *The Porphyrin Handbook*, ed. K. M. Smith, K. M. Kadish and R. Guillard, Academic Press, San Diego, 2000. (b) Dougherty, T. J; Gomer, C.; Henderson, B. W.; Jori, G; Kessel, D.; Kobrelik, Moan, J. and Peng, Q. *J. Natl. Cancer Inst.*, 1998, 90, 889. (c) Bonnett, R. *J. Heterocycl. Chem.* 2002, 39, 455.
2. Sherman, W. M.; Allen, C. M.; and van Lier, J. E. *Methods Enzymol.* 2000, 319, 376.
3. P. Workman, P.; Maxwell, R. J; and Griffiths, J. R. *NMR Biomed.*, 1992, 5, 270.

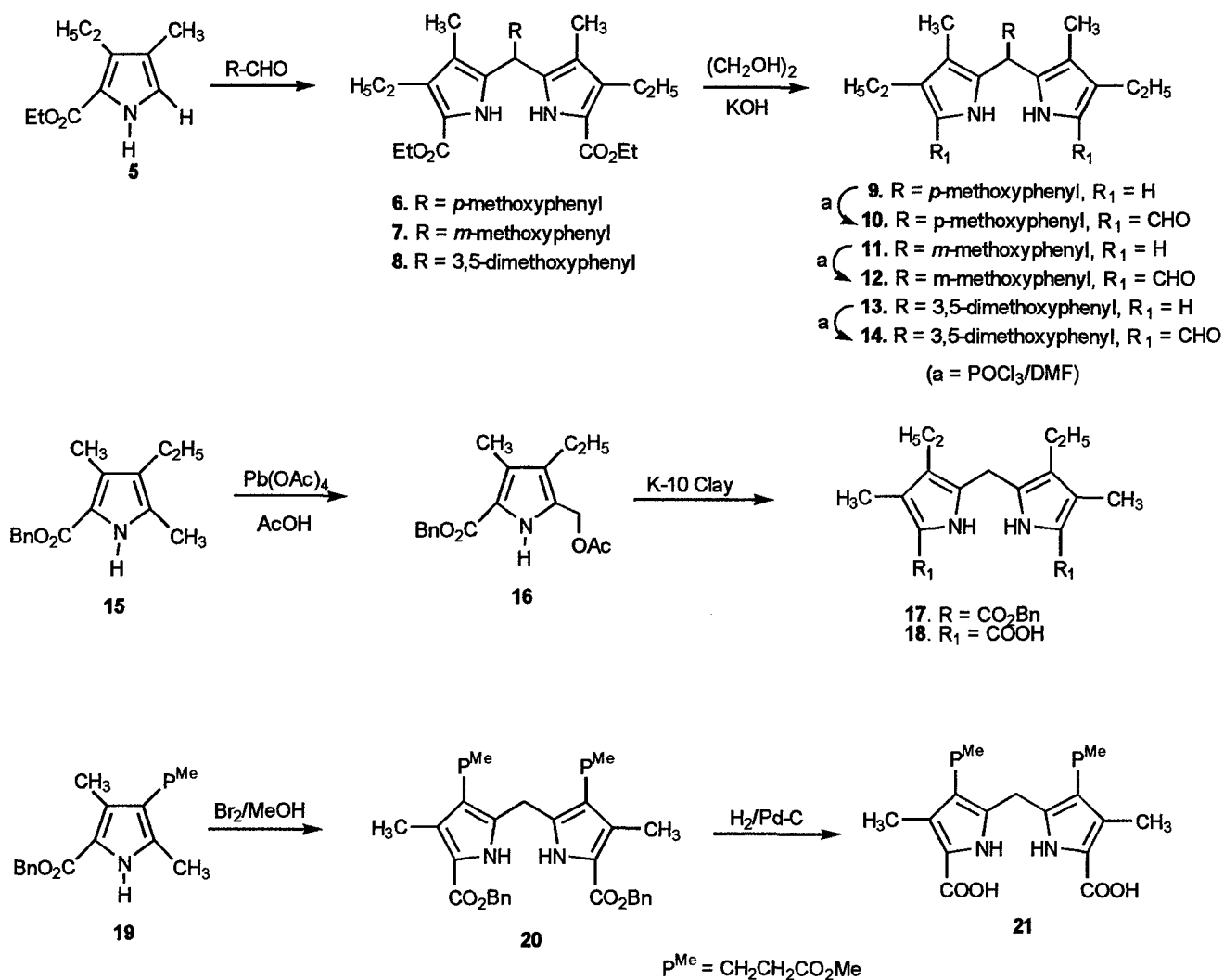
4. Bottomly, P. A. *Radiology*, **1989**, *170*, 1.
5. Mason, R. P.; Shukla, H. and Antich, P. P. *Magn. Reson. Med.*, **1993**, *29*, 296.
6. (a) Ceckler, T. L.; Gibson, S. L.; Hilf, R. and Bryant, R. G. *Magn. Reson. Med.*, **1990**, *13*, 416. (b) C. Thomas; Counsell, C.; Wood, P.; Adams, G. *Bull. Cancer*, **1993**, *80*, 666.
7. Jameson, C. J. in *Fluorine*, ed. J. Mason, Chapter 16, Plenum, New York, **1987**, 437.
8. Omote, M.; Ando, A.; Takagi, T.; Koyama, M. and Kumadaki, I. *Tetrahedron*, **1996**, *52*, 13961.
9. Barton, D. H. R.; Zard, S. Z. *J. Chem. Soc. Chem. Commun.* **1985**, 1098.
10. J. A. S. Caveleiro, J. A. S.; Gonsalves, A. M. d'A R; Kenner, G. W. and Smith, K. M. *J. Chem. Soc. Perkin Trans.*, **1973**, 240.
11. Jackson, A. H.; Smith, K. M. in *The Total Synthesis of Natural Products*, ed. J. ApSimon, Wiley, New York, **1973**, vol. 3, p. 144 and *1984*, vol. 6, p. 23.
12. Arsenault, G. P.; Bullock, E. and MacDonald, S. F. *J. Am. Chem. Soc.*, **1960**, *82*, 4384.
13. Clezy, P. S.; Fookes, C. J. R. and Liepa, A. J. *Aust. J. Chem.* **1977**, *30*, 2017.
14. (a) Pandey, R. K.; Jackson, A. H. and Smith, K. M. *J. Chem. Soc. Perkin Trans 1*, **1991**, 1211. (b) Smith, K. M. and Pandey, R. K. *Tetrahedron Lett.*, **1986**, *27*, 2717. (c) Jackson, A. H.; Pandey, R. K.; Rao, K. R. N. and Roberts, E. *Tetrahedron Lett.*, **1985**, 793.
15. Smith, K. M. in *The Porphyrins and Metalloporphyrins*, ed. K. M. Smith, Elsevier Sci. Amsterdam, **1975**.
16. Fukuzumi, S.; Suenobu, T.; Patz, M.; Hirasaka, T.; Itoh, S.; Fujitsuka, M. and Ito, O. *J. Am. Chem. Soc.*, **1998**, *120*, 8060.
17. Arbogast, J. W.; Darmanyan, A. P.; Chrostophor, P. D.; Foote, S.; Rubin, Y.; Diederich, F. N.; Alvarez, M. M.; Anz, S. J. and Whetten, R. L. *J. Phys. Chem.*, **1991**, *95*, 11.
18. Felton, R. H. in *The Porphyrins*, ed. D. Dolphin, Academic Press: New York, **1978**, vol. 5, Chapter 3.
19. (a) Pandey, R. K.; Sumlin, A. B.; Potter, W. R.; Bellnier, D. A.; Henderson, B. W.; Constantine, S.; Aoudia, M.; Rodgers, M. A. J.; Smith, K. M. and Dougherty, T. J. *Photochem. Photobiol.*, **1996**, *63*, 194. (b) Henderson, B. W.; Bellnier, D. A.; Graco, W. R.; Sharma, A.; Pandey, R. K.; Vaughan, L.; Weishaupt, K. R. and Dougherty, T. J.

- Cancer Res.*, **1997**, *57*, 4000. (c) Zheng, G.; Potter, W. R.; Camacho, S. H.; Missert, J. R.; G. Wang, G.; Bellnier, D. A.; Henderson, B. W.; Rodgers, M. A. J.; T. J. Dougherty, and Pandey, R. K. *J. Med. Chem.*, **2001**, *44*, 1540.
20. Pandey, R. K.; Potter, W. R.; Meunier, I.; Sumlin A. B. and Smith, K. M. *Photochem. Photobiol.*, **1995**, *62*, 764.
 21. Li, G.; Graham, A.; Potter, W. R.; Grossman, Z. D.; Oseroff, A.; Dougherty, T. J. and Pandey, R. K. *J. Org. Chem.*, **2001**, *66*, 1316.
 22. Chen, Y.; C.; Medforth, C. J.; Smith, K. M.; Alderfer, J. L.; Dougherty, T. J. and Smith, K. M. *J. Org. Chem.*, **2001**, *66*, 3930.
 23. Twentyman, PR; Brown, JM; Gray, JW; Franko, AJ; Scoles, MA; Kallman, RF. *J. Natl. Cancer. Inst.*, 1980, *64*, 595.

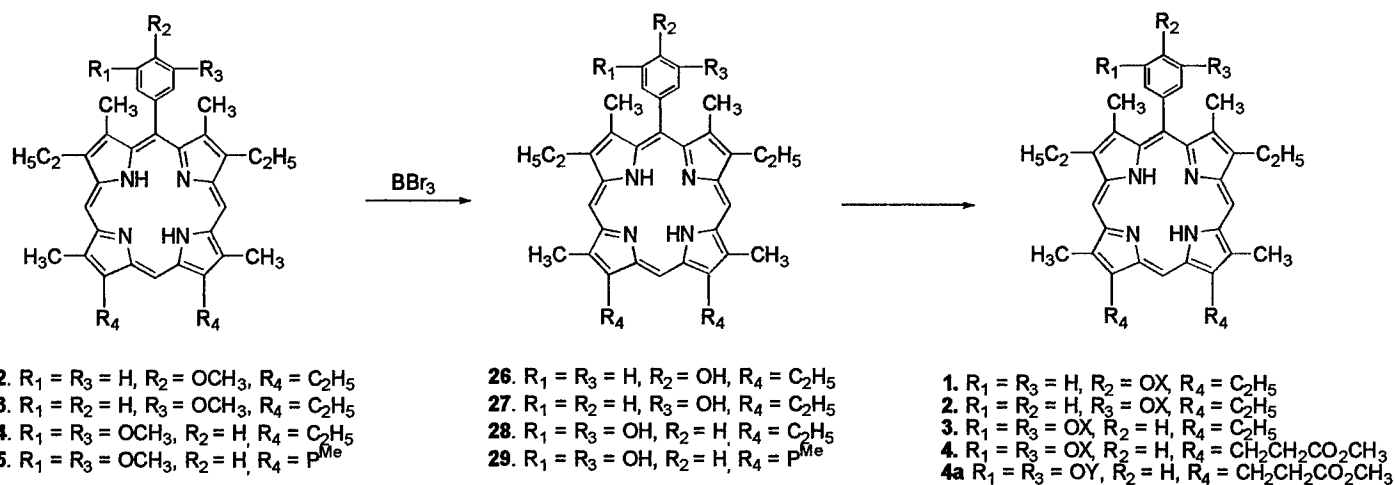


$pMe = -CH_2CH_2CO_2CH_3$
4 $R = CF_3$
4a $R = CH_3$

Chart-1

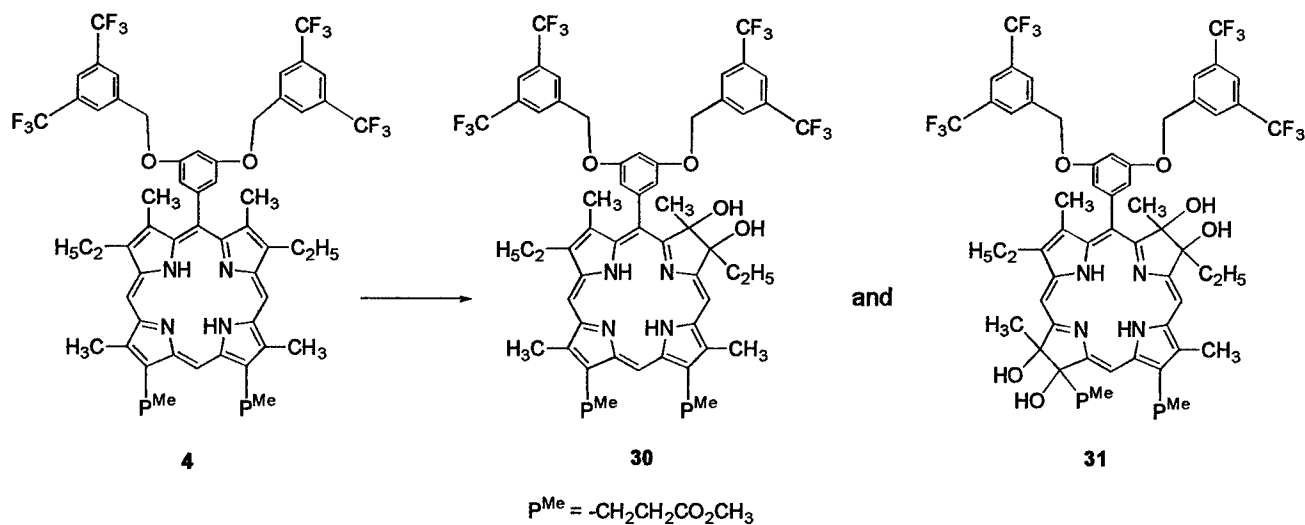


Scheme-1



Scheme-2

[X = -3,5-trifluoromethyl) benzyl]
[Y = 3,5-dimethyl)-benzyl]



Scheme-3

Table 1. Fluorescence emission maxima and fluorescence emission lifetime in deaerated PhCN at 298 K, and phosphorescence emission maxima in deaerated 2-MeTHF at 77 K

	λ_{max} (fluorescence)		τ (fluorescence) ^b	λ_{max} (phosphorescence)
	nm		nm	nm
26	628	693	18.5	822
27	627	693	17.9	822
28	628	693	17.3	822
29	628	692	17.6	823
1	628	693	18.6	823
2	627	692	16.1	823
3	628	693	18.5	822
4	628	691	17.7	822
4a	629	693	18.2	822
30	652	a	3.8	842
31	720	a	3.3	806

^a shoulder peak. ^b The experimental errors are within $\pm 5\%$.

Table 2. T-T absorption maxima ($\lambda_{\text{max}}(\text{T-T})$), triplet lifetimes ($\tau(\text{T-T})$) in the deaerated PhCN at 298 K, quenching rate constant of the triplet excited state by oxygen in PhCN, and quantum yield of singlet oxygen in C_6D_6 .

	$\lambda_{\text{max}}(\text{T-T})$, nm	$\tau(\text{T-T})$, s ^a	k_{EN} , $\text{M}^{-1} \text{s}^{-1}$ ^a	$\Phi(^1\text{O}_2)$ ^a
26	450	1.0×10^{-5}	9.4×10^8	0.26
27	450	1.1×10^{-5}	1.1×10^9	0.57
28	450	1.1×10^{-5}	1.0×10^9	0.68
29	450	1.1×10^{-5}	8.9×10^8	0.33
1	450	8.3×10^{-6}	9.9×10^8	0.61
2	450	1.4×10^{-5}	9.0×10^8	0.75
3	450	1.9×10^{-5}	1.0×10^9	0.81
4	450	2.5×10^{-5}	1.0×10^9	0.36
4a	450	2.3×10^{-5}	9.7×10^8	0.27
30	440	1.9×10^{-4}	1.1×10^9	0.30
31	440	7.7×10^{-5}	1.1×10^9	0.31

^a The experimental errors are within $\pm 5\%$.

Table 3. Reduction potentials of investigated complexes and UV-visible spectral data of singly reduced compounds in PhCN containing 0.1 M TBAP.

group	cpd	potential (V vs SCE)		singly reduced complexes			
		$E_{1/2}$	E_p	$\lambda_{\max, \text{nm}} (\epsilon \times 10^{-4} \text{ M}^{-1} \text{ cm}^{-1})$			
I	1	-1.43	-1.78	409 (6.1)	432 (4.9) ^{sh}	--	806 (0.7)
	2	-1.38	-1.80	408 (5.7)	435 (3.7) ^{sh}	--	813 (1.0)
	3	-1.40	-1.80	407 (4.3)	--	--	801 (0.9)
	4	-1.29	-1.66	412 (7.1)	--	--	801 (1.1)
II	26	-1.44	-1.68	410 (6.8)	434 (6.3)	--	799 (1.8)
	27	-1.44	-1.62	409 (5.1)	437 (4.1)	--	800 (1.9)
	28	-1.49	-1.66	409 (5.7)	439 (2.8)	--	800 (1.0)
	29	-1.46 ^a	-1.66	408 (5.2)	439 (2.5) ^{sh}	--	800 (1.2)
III	30	-1.30	-1.74	402 (3.5)	--	535 (0.7)	735 (1.2)
	31	-1.46 ^b	-1.84	406 (6.8)	--	750 (0.8)	827 (0.8)

^a E_p at a scan rate of 0.1 V/s. Two small peaks at $E_p = -0.52$ and -0.94 V also can be seen on first scan.

^b A peak at $E_p = -1.29$ V also can be seen.

sh = shoulder peak

Table 4. UV-visible data of investigated compounds, in PhCN containing 0.2 M TBAP.

group	compound	λ_{max} , nm ($\epsilon \times 10^{-4}$, M ⁻¹ cm ⁻¹)				
		Soret band	visible bands			
I	4	408 (12.71)	503 (1.13)	536 (0.51)	572 (0.47)	626 (0.19)
	2	409 (11.23)	503 (0.74)	538 (0.60)	572 (0.74)	624 (0.29)
	3	407 (7.25)	503 (0.65)	535 (0.30)	571 (0.27)	625 (0.10)
	1	407 (13.12)	503 (1.29)	535 (0.62)	572 (0.58)	625 (0.28)
II	26	407 (16.20)	504 (1.24)	536 (0.27)	573 (0.23)	624 (0.09)
	27	407 (12.47)	503 (0.48)	535 (0.20)	572 (0.16)	624 (0.10)
	29	412 (12.70)	504 (0.57)	538 (0.74)	570 (0.95)	615 (0.21)
	28	407 (9.58)	503 (0.88)	535 (0.40)	572 (0.37)	624 (0.15)
III	30	402 (8.28)	501 (0.79)	548 (0.17)	593 (0.26)	648 (2.12)
	31	399 (8.90)	506 (1.28)	593 (0.35)	645 (2.02)	715 (1.70)

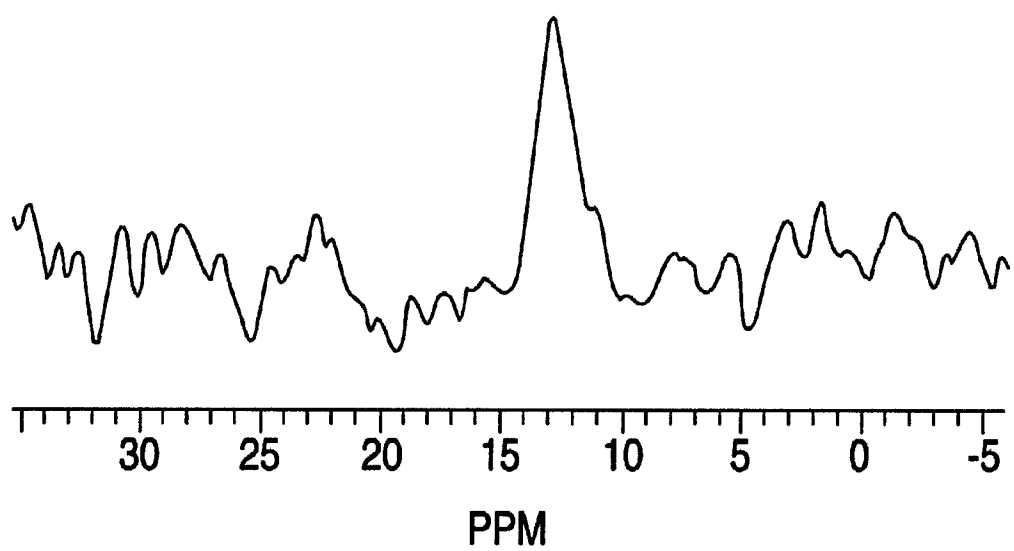


Figure 1

Figure 2

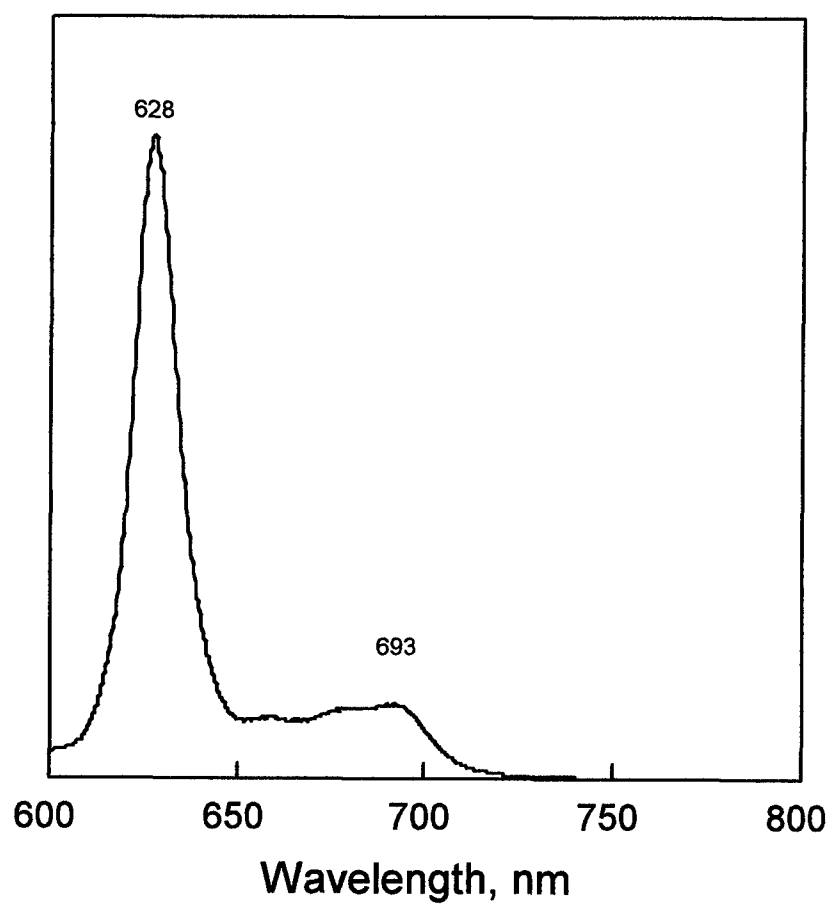


Figure 3

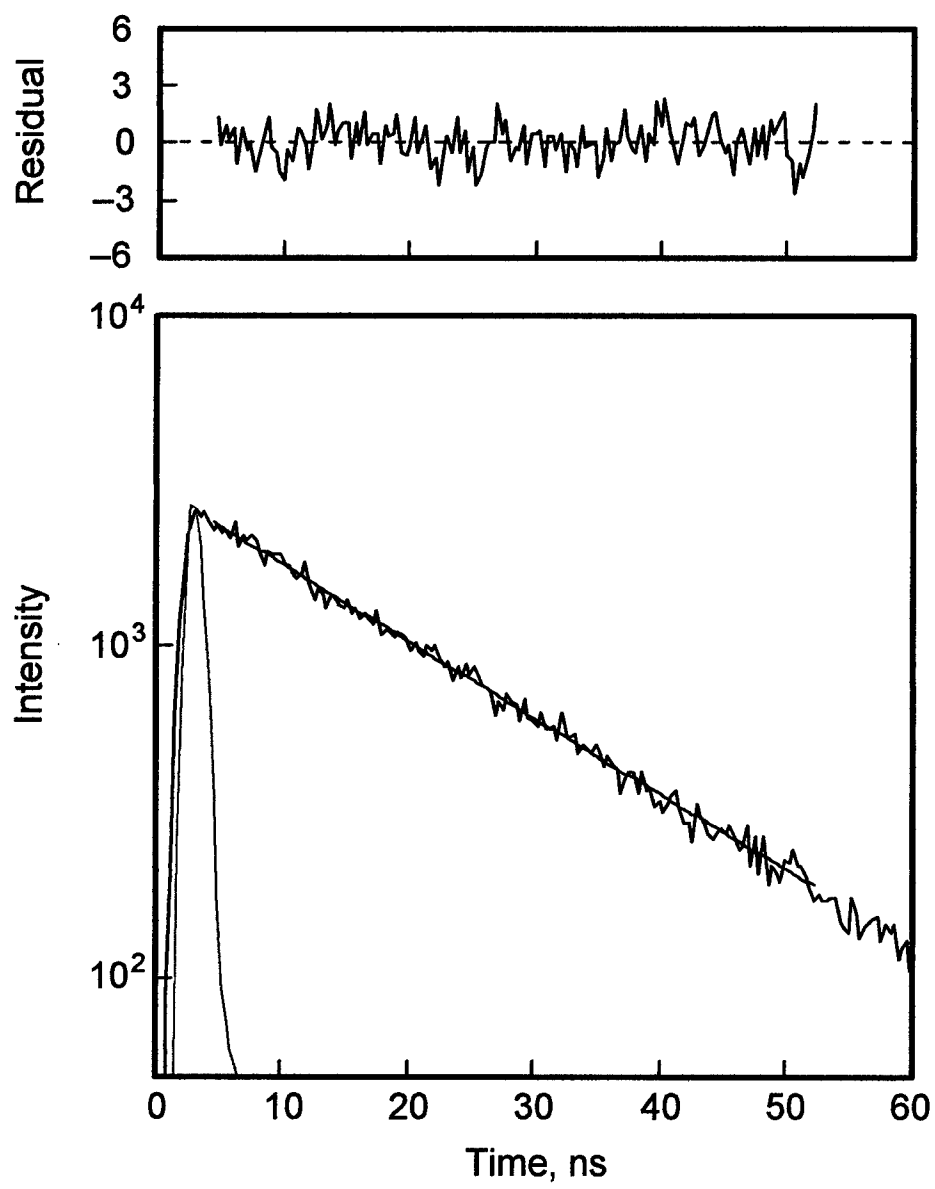


Figure 4

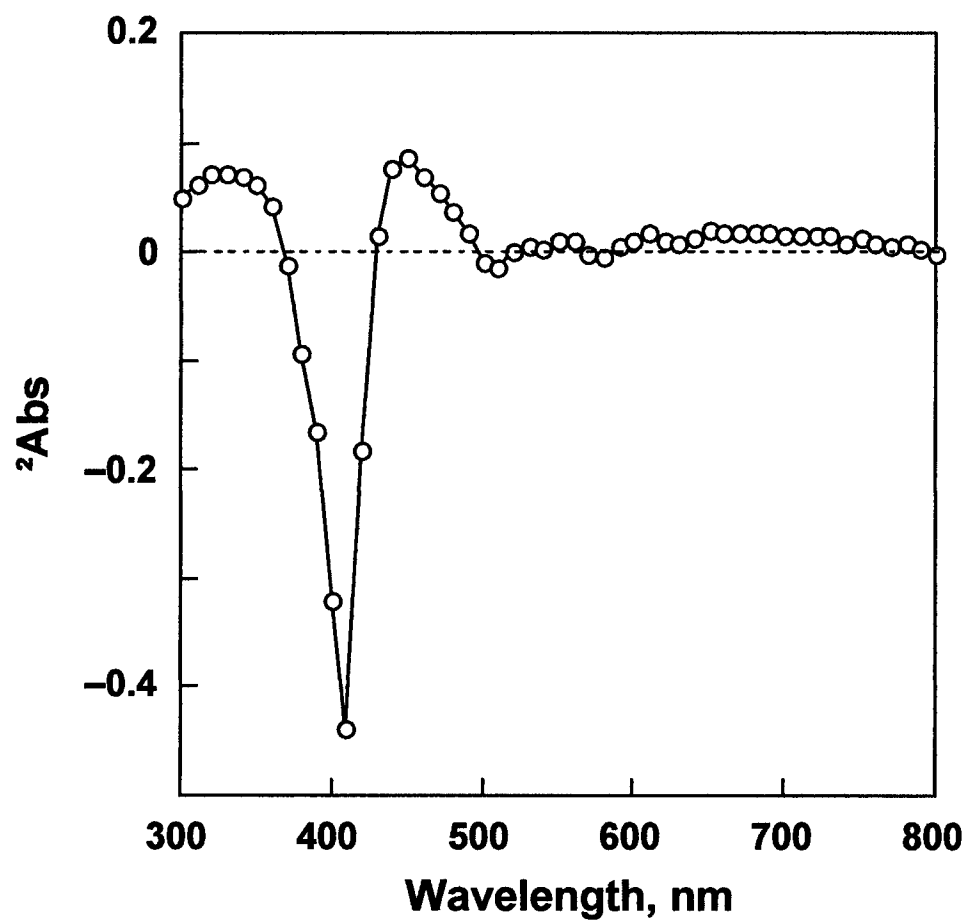


Figure 5

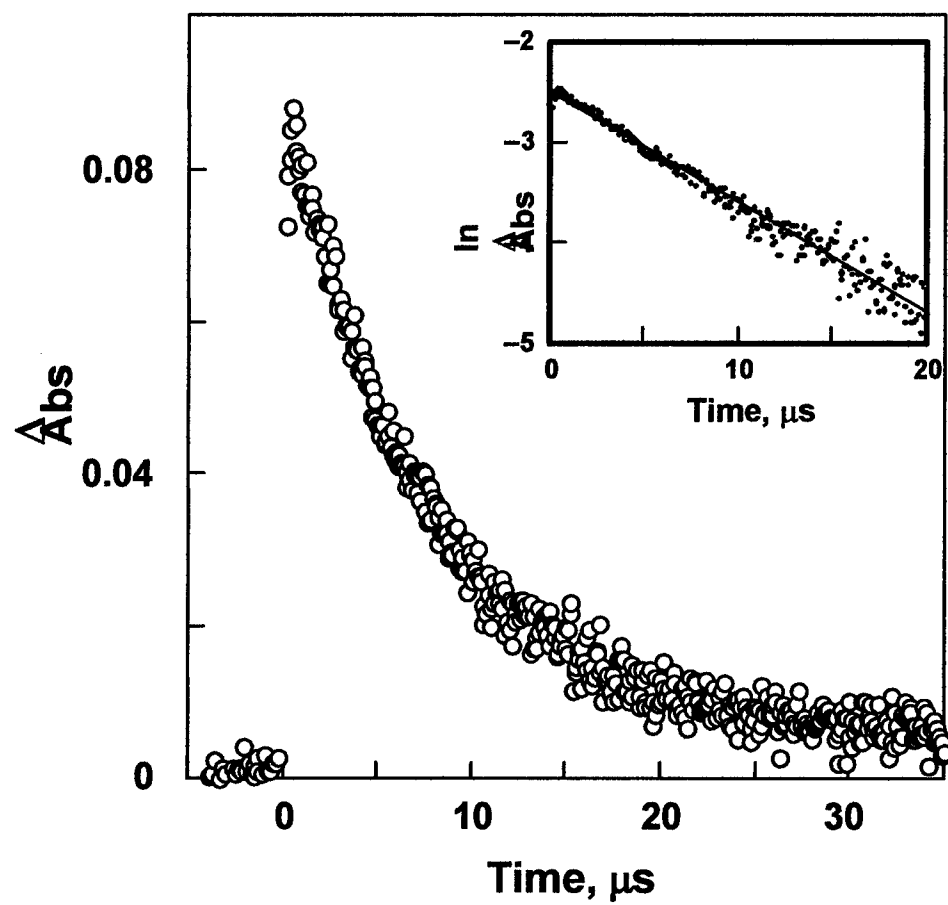
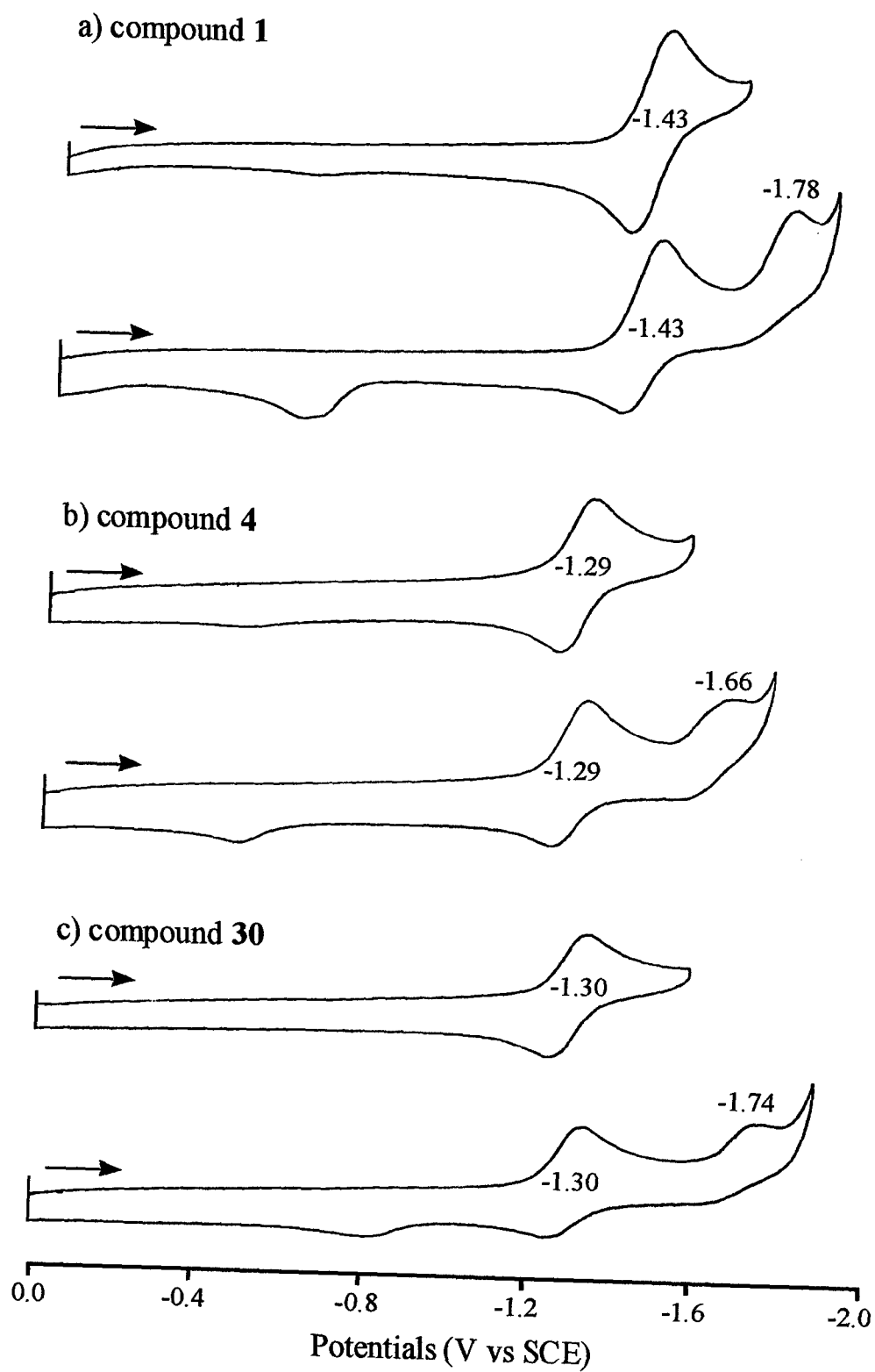
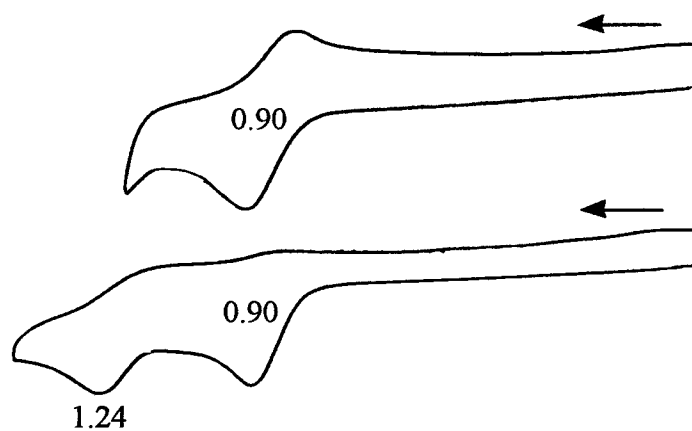


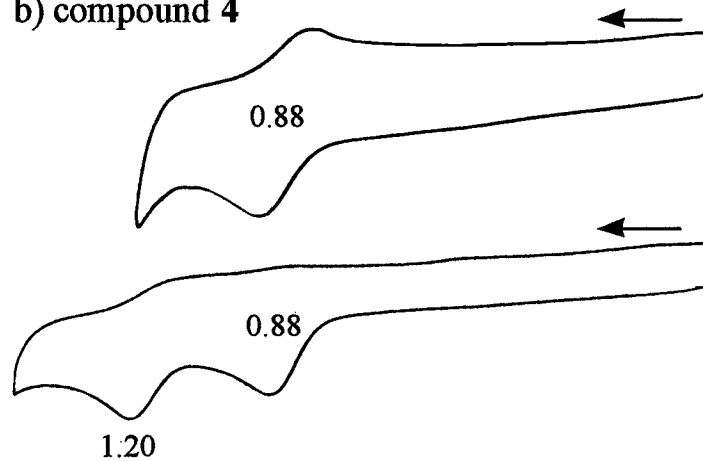
Figure 6



a) compound 3



b) compound 4



c) compound 30

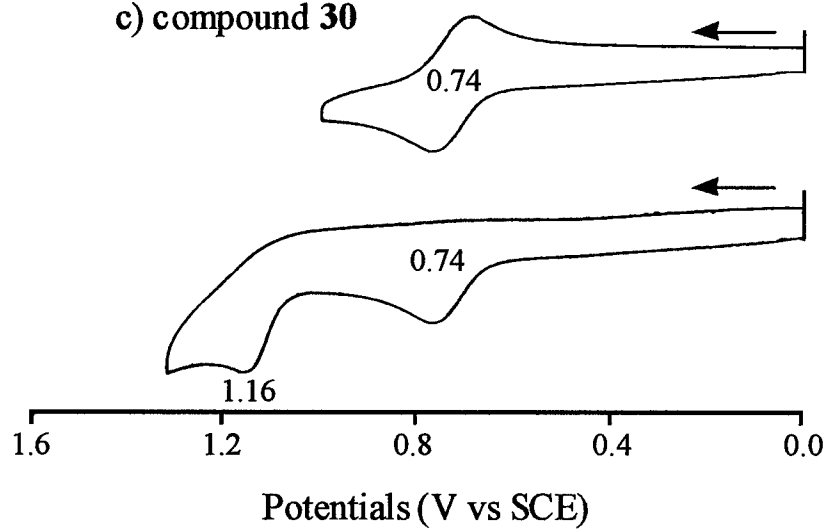


Figure 7

Figure 8

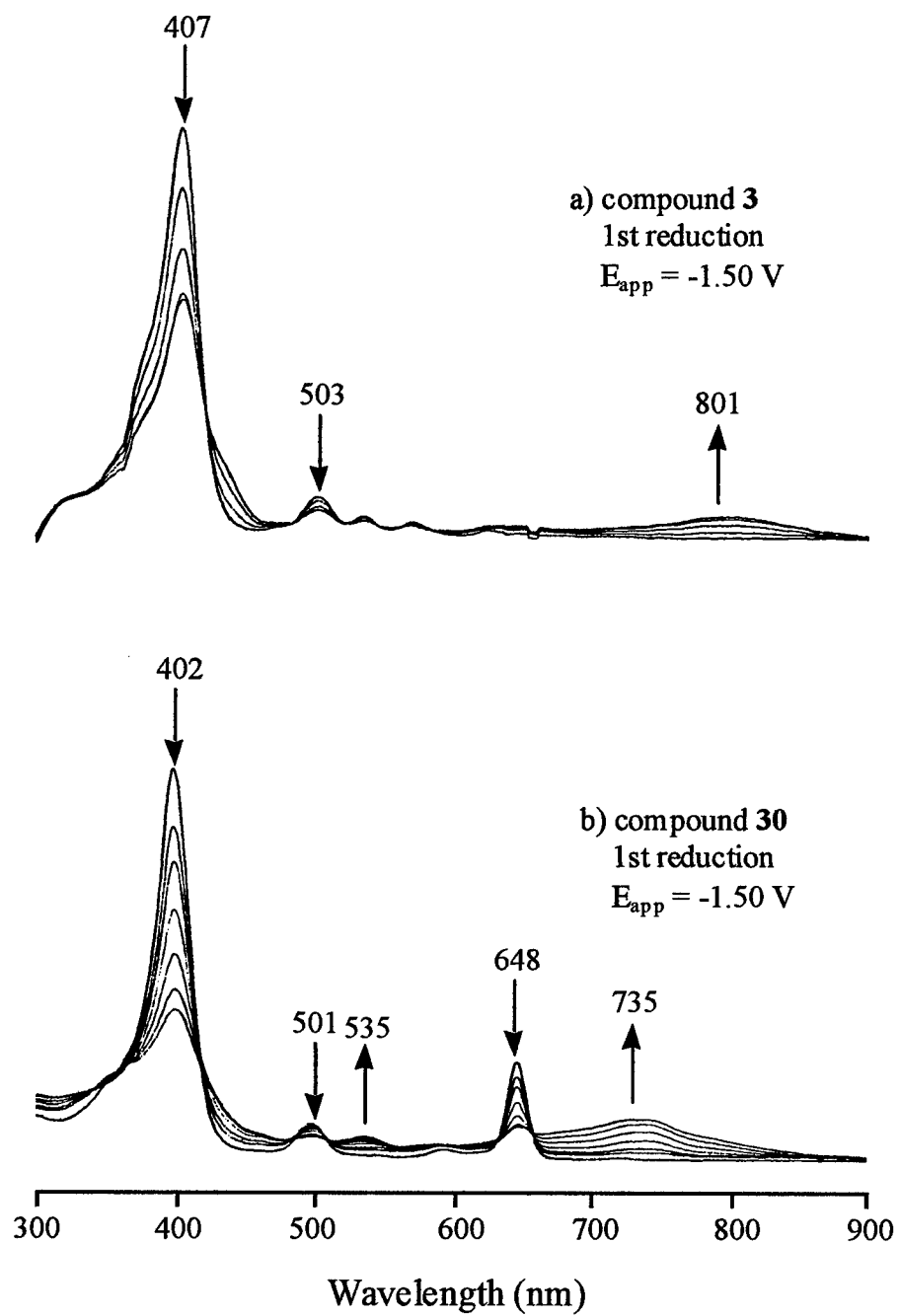


Figure 9

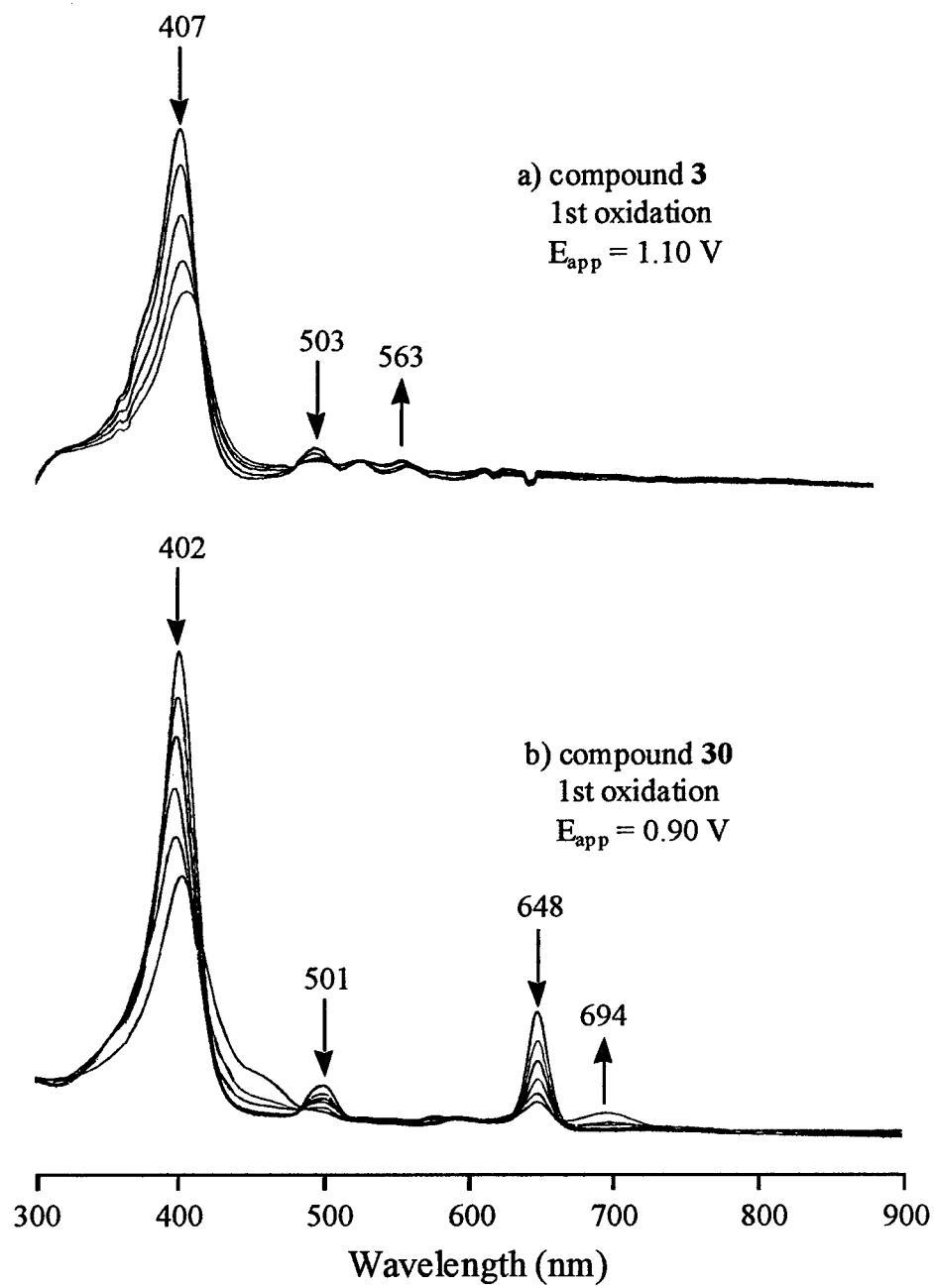


Figure 10

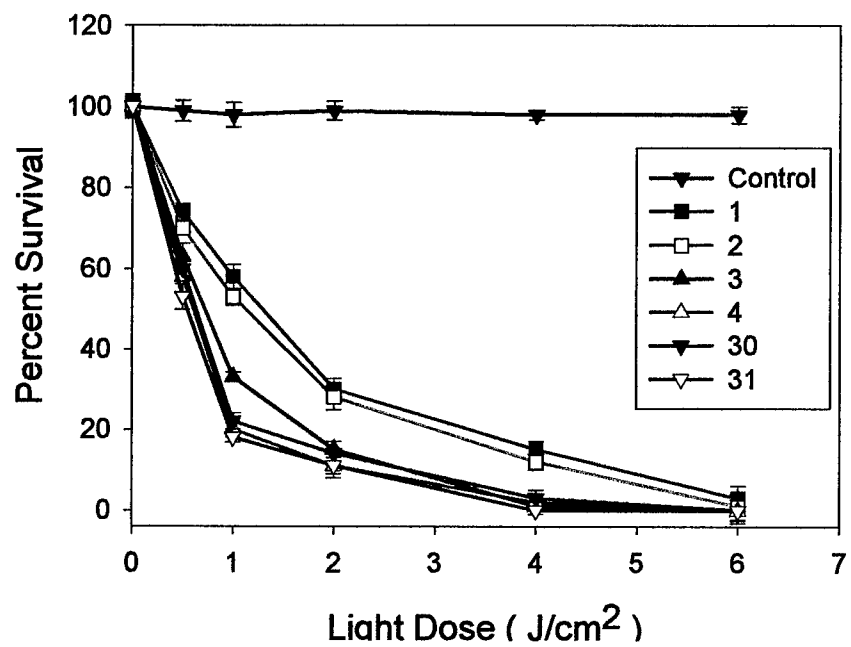
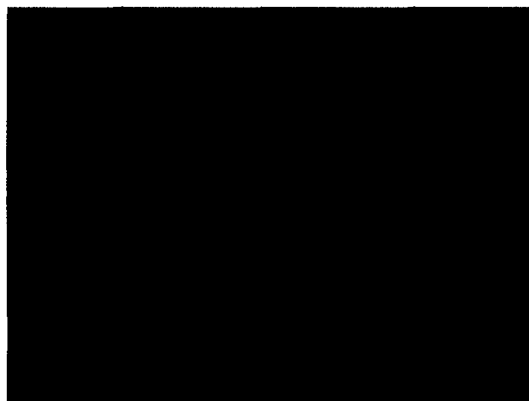


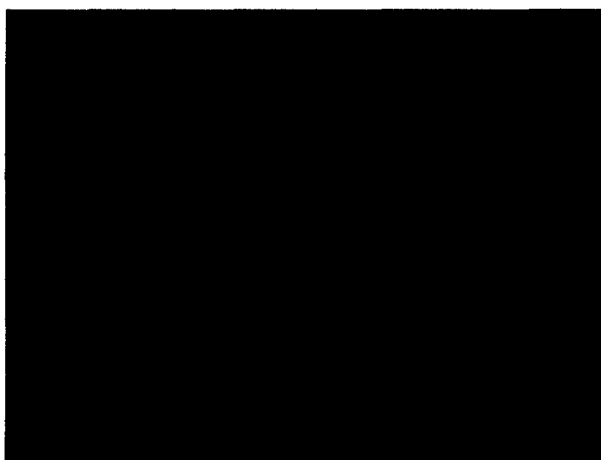
Figure 11



Rhodamine 123



Chlorin 30



Overlay

Figure Captions

Figure 1. In vivo ^{19}F NMR spectrum of compound **4** obtained from a RIF tumor implanted in a mouse (C3H/HeJ) foot dorsum in the hind leg.

Figure 2. Fluorescence spectrum of **3** (7.3×10^{-6} M) in deaerated PhCN at 298 K by excitation at 535 nm.

Figure 3. Fluorescence decay ($\lambda_{\text{em}} = 628$ nm) of **3** (7.3×10^{-6} M) in deaerated PhCN at 298 K by excitation at 535 nm. The instrument response (gray line), decay data (solid line), and single-exponential fitted line are plotted in the bottom frame. The residuals of the fit for a lifetime of $\tau = 18.5$ ns are plotted in the top frame.

Figure 4. T-T absorption spectrum of **3** (7.3×10^{-6} M) obtained by the laser flash photolysis in deaerated PhCN at 4.0 μs after laser excitation (355 nm) at 298 K.

Figure 5. Kinetic trace for the T-T absorption of **3** (7.3×10^{-6} M) at 450 nm in deaerated PhCN after laser excitation (355 nm) at 298 K. Inset: First-order plot.

Figure 6. Cyclic voltammograms illustrating the stepwise reductions of compounds a) **1**, b) **4** and c) **30** in PhCN containing 0.1 M TBAP.

Figure 7. Cyclic voltammograms illustrating the stepwise oxidation of compounds a) **1**, b) **4** and c) **30** in PhCN containing 0.1 M TBAP.

Figure 8. Thin - layer UV-visible spectral changes of a) compound **3** and b) compound **30** upon the first reduction at -1.50 V in PhCN containing 0.2 M TBAP.

Figure 9. Thin - layer UV-visible spectral changes of a) compound **3** and b) compound **30** upon the first oxidation at 1.10 and 0.90 V in PhCN containing 0.2 M TBAP.

Figure 10. The *in vitro* photosensitizing activity of various fluorinated porphyrins **1-3**, chlorin **30** and bacteriochlorin **31** (2 μ M) in RIF tumor cells at 24 h incubation. Control: Cell exposed to light without photosensitizer and cells with photosensitizer but no light exposure.

Figure 11: Comparative intracellular localization of Rhodamine 123 (mitochondrial probe) and fluorinated chlorin **30** in RIF cells at 24 h post-incubation. Similar patterns were observed from fluorinated porphyrin **4** and the corresponding bacteriochlorin **31** (only a representative example is shown). The overlay picture clearly indicates that both Rhodamine 123 and chlorin **30** localize in mitochondria.

Table 1. Fluorescence emission maxima and fluorescence emission lifetime in deaerated PhCN at 298 °K, and phosphorescence emission maxima in deaerated 2-MeTHF at 77 °K

Appendix-C

**Curriculum Vitae of participants who were trained during the
past two years**

- a. Elzbieta Rzepka -- Undergraduate level**
- b. Jiaxiong Pi ----- Graduate level**
- c. Mahabir Dobhal— Postdoctoral level**

ELZBIETA RZEPKA
8061 Martha St
Omaha, NE 68124
(402) 392-2683

EDUCATION

University of Nebraska at Omaha, Omaha, NE
Bachelor of Science – Biology Major
Senior who is scheduled to
Graduate summer of 2003

Relevant Courses include:

Biology I & II	Genetics
Microbial Physiology	General Chemistry I & II
Molecular Biology of the Cell	Developmental Biology
Organic Chemistry	Endocrinology

Westside High School, Omaha, NE
Graduating class of 1998

Relevant Courses include:

Biology	Chemistry
Physics	

**WORK
EXPERIENCE**

July 1998 -
November 2001

The Sitar Restaurant
Waitress

November 2001-
Present

University of Nebraska Medical Center
Lab Technician

References

A. Thomas Weber
Department of Biology
University of Nebraska at Omaha
6001 Dodge St.
Omaha, NE 68182-0040
tweber@unomaha.edu
Phone: (402) 554-2619
Fax: (402) 554-3532

Dan M. Sullivan, Ph.D.
Department of Chemistry
University of Nebraska at Omaha
6001 Dodge St.
Omaha, NE 68182-0109
sully@unomaha.edu
Phone: (402) 554-3646
Fax: (402) 554-3888

ACTIVITIES

Nebraska Humane Society volunteer

Saint Margaret Mary's Church volunteer

Salvation Army volunteer

Presentations

Research Colloquium Poster Session on

"In Vivo Magnetic Resonance Measurements of Lithium in Rat Hind Limb" Presented at the University of Nebraska Medical Center, August 2002

"MR Determination of Lithium in Plasma and RBC of Small Blood samples." Presented at the University of Nebraska Medical Center, August 2002

"The Effects of Fluoxetine on Lithium Blood Levels in Rats." Presented at the University of Nebraska Medical Center, August 2002.

Pharmacokinetics and relaxivity of Lithium in Rat Thigh Muscle by MR Studies

E. Rzepka¹, S. Ramaprasad¹, Presented at the 11th ISMRM Scientific Meeting, Toronto, Canada, 2003

Codrug Effects on Lithium in an Animal Model by ⁷Li MR.

By: K. Luterbach¹, E. Pierson¹, E. Rzepka¹, S. Ramaprasad¹
Presented at the ISMRM Scientific Meeting, Toronto, Canada, 2003

In Vivo ¹⁹F MR Studies of Fluorine Labeled Photosensitizer in Murine Tumor Model. S. Ramaprasad¹, E. Rzepka¹, S.S. Joshi², M.P. Dobhal³, J. Missert³, R.K. Pandey³, To be presented at the ESMRMB Scientific Meeting, at De Doelen Congress Center, Rotterdam, September 2003.

Objective:

To become familiarized and to gain experience in the research field especially pertaining to Breast cancer studies.

Employment Background:

At University Medical Center at Omaha

Cell Culture

Maintained four different lines of cells. SKBR 3, MRA 231, and MRA453 all breast cancer cells. The three lines of breast cancer cells were maintained from November of 2001 the end of the year. Currently maintaining RIF-1 cells received from Roswell Park Cancer Inst. The RIF-1 cells are being maintained since Feb. 2002.

Doubling time

Finding out the doubling time of RIF-1 cells was accomplished with the use of the fisher scientific hemocytometer.

Freezing and thawing of cells

I am experienced in freezing all four lines of cells listed above. Method: mix a fifty to fifty solution containing media and cryoprotectant media then dilute your cells in this and put one ml in each container. I have also started culturing RIF-1 cells from a frozen sample that was brought in from Roswell Park Cancer Institute.

Growing and maintaining RIF-1 tumors

I have injected RIF-1 cells into C3h/Hej mice both on the flank and also on the dorsal side of the foot. Once tumors were visible I kept track of the tumor volumes and made sure tumors stayed within a specific growth window. If the volume got too extensive I put the animal down.

Numbering of mice

I have weighed and numbered around thirty mice. Procedure: by piercing their ears using a ear piercing code; five mice were kept per cage in special micro isolators.

Numbering of rats

I have weighed and numbered around eighty rats. Procedure: writing the number on the rats tail with a magic marker. This process worked well as long as the animal only needed to be kept track of for a couple of weeks.

Drawing blood from rats and mice

I have drawn blood from around thirty rats. Method used was to anesthetize them, make sure animal was sedated by lightly pinching their foot. Once this was accomplished the blood was drawn from the heart. .8-1.4 ml of blood was extracted from the animals. To keep the blood from clotting one ml of an anticoagulant solution was added. Recently just started extracting blood from mice. I have drawn blood from a couple mice. Generally around one ml of blood can be drawn from a mouse. Same method followed as in the rat procedure.

Anesthetizing small animals

I am in the process of using two methods of anesthetics. The first is generally used before the blood drawing. This method is a cocktail of Ketamine and Xylazine that is injected into the thigh region of a rat.

The second method is by using an anesthetizing machine containing isoflurane of 1.5, N2O at 600 cc/min., and O2 at 200 cc/min. The rats are anesthetized in two to five minutes. This method of anesthetizing is generally used before and during MRI studies and also when the cocktail of Ketamine and Xylazine is not available.

Brain extraction

I have extracted neural tissue from more than eighty rats. Method used : The animal is laid on its back and with a pair of dull tipped scissors you make an incision through the throat area and cut through the bone. Then pull back the skin till the skull is exposed you then make to incisions on both sides and cut along the sides of the skull. Once the neural tissue is exposed you lightly go around with a spatula to loosen and release the neural tissue from its cavity.

Photo Spectrometry

I am experienced in the use of a Bio Spec 1601 to find different wavelengths of photofrin solutions, which are currently being used on RIF-1 tumor cells.

MRI Studies

I have run a couple rat blood studies relating to Li levels in RBC and plasma I have gained experience in performing preliminary MRI and MRS studies relating with lithium distribution in a rats thigh. I also integrated spectral data for quantitating the tissue lithium. I am also involved in various data processing related to ^{19}F spectroscopy of murine tumors.

I also supervised the animals breathing rate and their levels of anesthetic during the experiments.

Using laser for PDT studies

Recently I have participated and performed experiments using a laser C3H/HeJ mice bearing tumors on the foot or on the flank.

CD Backup

I periodically transfer the MRI/MRS data and back them up on CD's using the Unix C Shell operating system.

Jiaxiong Pi

Address:

7070 Capitol Court, #678

Omaha NE, 68132

E-mail: jpi@mail.unomaha.edu

Homepage: <http://www.geocities.com/pijx/>

Objective:

To obtain an internship that will allow me to utilize my technical, communication, decision making and problem solving skills in a challenging research environment.

Education:

University of Nebraska at Omaha

January 2002-current

The Peter Kiewit Institute

M.S. Computer Science

Specialized in Networking and Communication

GPA: 3.7/4.0

Anticipated Degree Date: May 2004

Dalhousie University

September 1999-August 2001

Halifax, Canada

M.S. Atmospheric Sciences

GPA: 4.0/4.0

Degree Date: August 2001

Lanzhou University

September 1990-June 1994

Lanzhou, China

B.S. Atmospheric Physics & Atmospheric Environment

GPA: 3.8/4.0

Degree Date: June 1994

Work Experience:

University of Nebraska Medical Center

Department of Radiology-Dr. Ramaprasad

May 2003 - present

- Part time student researcher
collect and analyze MR spectrum data,
will be involved in pulse programming

University of Nebraska at Omaha

August 2002- Dec. 2002

College of Information Science and Technology

- Developed a web front-end accessed
Equipment, Maintenance,
User Tracking (EMU) System
(ASP and Access)

University of Nebraska-Lincoln
Department of Architectural Engineering – Dr. Lily Wang
Part-time programmer

August-October 2002

- Developed audio play & evaluation system (Java)

University of Illinois at Urbana-Champaign

August-December 2001

- Research Assistant

Dalhousie University

September 1999-August 2001

Physics Department

Teaching Assistant/Research Assistant

- Teaching assistant for:
Physics 2500 – Oscillation and Wave,
Physics 3500 – Electromagnetism,
Physics 5000 – Cloud Physics
- Designed/developed shell scripts and Fortran programs to compute surface fluxes from SSM/I data and ECMWF data
- Familiar with scientific data format including NetCDF, HDF/CDF
- Arctic cloud modeling for international project – FIRE.ACE/SHEBA with GESIMA model
- Process signal images using PCI including ingestion, manipulation and basic analysis

Chinese Academy of Meteorological Sciences
Beijing, China

June 1994-August 1999

Assistant Researcher

- Process/analyze PMS data on PC
- Member of a research group –
“The Variation of Ice-Nuclei Variation in Beijing and Its Effect on Climate.”
- Precipitation Enhancement field campaign for drought relief in northern China

Qualifications:

- Good programming skill in C++, Java, Fortran, Shell Script, IDL, HTML, ASP and Prolog.
- Familiar with Unix, Window 2000/NT/XP and Linux
- Strong background in mathematics and physics
- Seven (7) years working experience in data processing and analysis on PC's, workstations and supercomputers
- Responsible, efficient, cooperative and eager to learn new technology

Honors:

- Awarded Lanzhou University scholarship four consecutive years
- Second Prize winner of General Physics contest held at Lanzhou University, 1990
- Third Prize winner of Advanced Mathematics contest held at Lanzhou University, 1991
- Ranked No. 2 in the final evaluation for 4 academic years in Lanzhou University.
- Recognized as an "Excellent Researcher" by Chinese Academy of Meteorological Sciences

Publications:

- U. Lohmann, J. Zhang and J. Pi, "*Sensitivity studies of the effect of increased aerosol concentrations and snow crystal shape on the snowfall rate in the Arctic*", J. Geophys. Res., 108(D11), 4341, doi:10.1029/2003JD003377, 2003.
- J. Pi and U. Lohmann, "*Anthropogenic Aerosol Effect On Arctic Precipitation-A Case Study With GESIMA Model*" Proceedings of 35th Canadian Meteorological and Oceanographic Society (CMOS) Conference, Page 99, 26-30 May, 2001
- J. Pi and U. Lohmann, "*Arctic Cloud Simulation With GESIMA Model- A Case Study*" International Cloud Modeling Workshop, 4-11 August, 2000, Glenwood Springs, Colorado
- L. You, S. Yang, X. Wang and J. Pi, "*A study of Variation Characteristic of Ice Nuclei Concentration in Thirty Years at Beijing*" Proceedings of 14th International Conference on Nucleation and Atmospheric Aerosols, 26-30 August, 1996, Helsinki, Finland, p330~333

References:*Reference 1:*

Lily Wang
Assistant Professor
Architectural Engineering Program
University of Nebraska at Lincoln
200B Peter Kiewit Institute,
Omaha NE 68182-0681

lwang4@unl.edu

(402) 554-2065 (office)

(402) 554-2080 (fax)

Reference 2:

Jong-Hoon (Jon) Youn
Assistant Professor
Department of Computer Science
University of Nebraska at Omaha
282E Peter Kiewit Institute
Omaha NE 68182-0681

jyoun@mail.unomaha.edu

(402) 554-2187 (office)

Curriculum -vitae

Name

Dr. Mahabeer Prasad Dobhal

PII Redacted

Educational Qualification

- B.Sc , from Agra University, Agra (1973)
- B.Ed., from Agra University, Agra (1974)
- M.Sc., from Garhwal University, Srinagar (1976)
- Ph.D. from University of Rajasthan , Jaipur (1982)

Research Experiences

1. ► August 1976 to February 1982 worked for Ph.D. degree on the project entitled Chemical Investigation of Medicinal Plants of Garhwal Region under the supervision of Prof. B.C. Joshi .
2. ► December 1982 to April 1983 worked as Post – Doctoral fellow with Prof. B.C. Joshi.
3. ► In May 1983 UGC Research Associateship was awarded , during this period, (May 1983 to August 1984) chemical investigation of some medicinal plants was carried and a few anti-epileptic agents were isolated.

Work Experiences

1. Worked as a Production Chemist in Navin Chemicals Ltd. NOIDA (India)
2. From September 1984 I have been working as an Assistant Professor in the Department of Chemistry , University of Rajasthan, Jaipur .

List of Publications

- | | | | |
|--|---|-----------------------------------|------|
| 1. Chemical investigation of <i>Roylea elegans</i> part-I | M.P. Dobhal
B.C. Joshi | Herba Polon, 25, 95 | 1979 |
| 2. Chemical investigation and biological screening of the stems of <i>Rhododendron anthopogon</i> | M.P. Dobhal
Y.C. Joshi
B.C. Joshi | Die Pharmazie 36, 381 | 1981 |
| 3. Studies of Potential heterocyclic sulphones as antimicrobial agents. Synthesis & antimicrobial activity of some novel substituted arylsulphonyl benzo (f) quinoline | R.P. Bahuguna,
Y.C. Joshi,
M.P. Dobhal,
B.C. Joshi,
H.N. Mangal | Heterocycles, 16,
1955 | 1981 |
| 4. Spectral studies of some substituted arylthiobenzo (f) quinolines | R.P. Bahuguna,
Y.C. Joshi, | J. Heterocyclic Chem.
5495, 66 | 1982 |

M.P. Dobhal,
R.K. Pande,
B.C. Joshi

5. Chemical constituents of the stems of *Roylea elegans* S. Ansari Y.C. Joshi, **M.P. Dobhal**, B.C. Joshi Die Pharmazie 37, 72 1982
6. Phytochemical investigation of the roots of *Colebrookia oppositifolia* S. Ansari **M.P. Dobhal** R.P. Tyagi B.C. Joshi F.S.K. Barar Die Pharmazie 37, 72 1982
7. Chemical investigation and Pharmacological screening of *Roylea elegans* Part-II S. Kumar, **M.P. Dobhal**, B.C. Joshi, F.S.K. Barar Herba Polon 27, 99 1982
8. Chemical investigation of the roots of *Anisomeles indica* S. Ansari, **M.P. Dobhal** Die Pharmazie 37, 453 1982
9. A review on genus *Rhododendron* **M.P. Dobhal**, Y.C. Joshi B.C. Joshi Herba Polon 29, 65 1983
10. Spectral and antimicrobial studies of some substituted arylthibenzo (h) quinolines R.P. Bahuguna, Y.C. Joshi, **M.P. Dobhal**, B.C. Joshi, H.N. Mangal J. Inst. of Chemists (India) 56, 185. 1984
11. Chemical investigation of various species of the plants belonging to *Berberdiaceae* **M.P. Dobhal** B.C. Joshi Rasayan Samiksha 2, 26 1986
12. Chemical investigation of aerial parts of *Portulacca sufruticosa* Y.P. Agrawal **M. P. Dobhal** Herba Polon 33, 71 1987
13. Chemical investigation of *Euonymus Pendulus* Characterization of a new isoflavone (Garhwalin) **M.P. Dobhal** Y.P. Agrawal B.C. Joshi Die Pharmazie 42, 558 1987
14. Chemical investigation of the seed coats of *Prunus amygdalus*. B.C. Joshi A.K. Chauhan, Herba Polon 33, 163 1987

- | | | | |
|--|---|--|------|
| Isolation and characterization of a new biflavone | M.P. Dobhal,
V.P. Agrawal | | |
| 15. A review on medicinal plants, showing anticonvulsant activity | A.K. Chauhan
M.P. Dobhal, | J. Ethnopharmacology
22, 11 | 1988 |
| 16. Phytochemical studies of stems of <i>Anisomeles indica</i> | M.P. Dobhal,
A.K. Chauhan,
S. Ansari,
B.C. Joshi | Fitoterpia 59, 155 | 1988 |
| 17. Chemical investigation of <i>Catalpa longissima</i> Part-I | A.K. Chauhan
M.P. Dobhal,
P.N. Uniyal | Herba Polon 34, 4 | 1988 |
| 18. Chemical investigation of <i>Berberis chitria</i> 'Ham' - Isolation and characterization of isoquinoline alkaloids | M.P. Dobhal,
V.K. Goel,
B.C. Joshi | Die Pharmazie 43,
659 | 1988 |
| 19. Chemical investigation and biological activity of <i>Berberis chitria</i> | M.P. Dobhal
G.S. Negi | Himalayan Chem. Pharma, Bull 5, 41 | 1988 |
| 20. Characterization of a new alkaloids from the roots of <i>Berberis chitria</i> | A.K. Chauhan
M.P. Dobhal | Die-Pharmazie 44, | 1989 |
| 21. Structure and activity relationship of isoquinoline alkaloids. | R.S. Gupta
V.P. Dixit,
M.P. Dobhal | Fitoterapia 61, 67 | 1990 |
| 22. Chemical constituents of the bark of <i>Euonymus echinatus</i> | A.K. Chauhan,
M.P. Dobhal,
Diwakar Sharma | Himalayan Chem. & Pharm.Bull. 6, 21 | 1989 |
| 23. A review on genus <i>Rhododendron</i> - Part II | M.P. Dobhal | Herba Polon 37, 89 | 1991 |
| 24. <i>In Vitro</i> antimicrobial efficacy of <i>Berberis chitaria</i> extracts | M.P. Dobhal
Y.C. Joshi | Fitoterapia 63, 69 | 1992 |
| 25. A new isoquinoline alkaloid from <i>Berberis chitria</i> | M.P. Dobhal,
A.K. Chauhan, | Indian Science Congress Assoc. | 1993 |
| 26. A Review on genus <i>Euonymus</i> | A.M. Hassan,
C. Kaushik
M.P. Dobhal | Herba Polon 41, | 1995 |

- | | | | |
|--|---|---|------------------------------|
| 27. A Review on genus <i>Eupatorium</i> Part-I | A.M. Hassan,
M.P. Dobhal
B.C. Joshi,
G.S. Negi | Him.Chem. &
Pharma Bull. 12, 1-10 | 1995 |
| 28. Synthesis of some new sulphide sulphone and triazolo derivatives of pyridobenzodiazepines | B.C. Joshi
R.P. Tyagi
Madhu Chauhan,
M.P. Dobhal | Indian J. of
Heterocyclic Chem.
5, 277-80 | 1996 |
| 29. A Review of the Chemical Constituents in the genus <i>Eupatorium</i> Part-II | A.M. Hassan,
M.P. Dobhal
G.S. Negi
B.C. Joshi | Himalayan Chem. &
Pharm. Bulletin 12 | 1996 |
| 30. Morphometric and biochemical changes in tests of <i>Presbytis entellus</i> (Langur) Followed by aristolochic acid administration | R.S. Gupta
M.P. Dobhal,
V.P. Dixit | Annals of Biology 12,
328-34. | 1996 |
| 31. A review on the chemical constituents in the genus <i>Eupatorium</i> - Part-III | A.M. Hassan,
M.P. Dobhal
G.S. Negi
B.C. Joshi | Himalayan Chem. &
Pharm. Bulletin 14, | 1997 |
| 32. A brief review on chemical constituents of some medicinally important species of Genus <i>Plumeria</i> | A.M. Hassan
B.C. Joshi
M.P. Dobhal | Asian J. of Chemistry
9, 571-78. | 1997 |
| 33. A review on cyclopeptide alkaloids | Chetan Kaushik
M.P. Dobhal | Himalayan Chem. &
Pharm. Bulletin 15,
22-32 | 1998 |
| 34. Ferulic acid ester from <i>Plumeria bicolor</i> | M.P. Dobhal
A.M. Hasan
M.C. Sharma
B.C. Joshi | Phytochemistry 51,
319-21 | 1999 |
| 35. Effects of coumarin derivatives on testicular population in Langur monkeys. | R.S. Gupta,
V.P. Dixit
M.P. Dobhal | Himalayan Chem. &
Pharm. Bulletin. | 1999 |
| 36. Antifertility studies and Chemical investigation of <i>Colebrookia oppositifolia</i> leaf extract in male albino rats. | R.S. Gupta
R.K. Yadav,
V.P. Dixit, | Fitoterapia | 1999
Accepted
In Press |

M.P. Dobhal

- | | | | |
|---|--|--------------------------------------|------|
| 37. Antifertility studies of the root extract of the <i>Barlaria prionitis</i> in male albino rats with special reference to testicular cell population dynamics. | R.S. Gupta
P. Kumar,
V.P. Dixit,
M.P. Dobhal | J. Ethnopharmacology
70, 111-17 | 2000 |
| 38. Effect of Organoantimony Compounds sterically hindered bifunction legands on the reproductive systems. | R.K. Sharma
M.P. Dobhal ,
Y.P. Singh,
R.S. Gupta | Metal Based Drugs
7, 271-74 | 2000 |
| 39. Hypocholeserolemic effect of the oleoresin (<i>Capsicum annum</i>) in gerbils. | R.S. Gupta
V.P. Dixit,
M.P. Dobhal | Phytotherapy Research
15, 1-3, | 2001 |
| 40. Effect of Alstonia scholaris bark extract on testicular function of Wistar rats | R.S. Gupta
M.P. Dobhal | Asian J. Andrology
4, 175 – 78 | 2002 |
| 41. Antispermatogetic effect and chemical investigation of <i>Opuntia dillenii</i> | R.S.Gupta
A.Sharma
M.P. Dobhal | Pharmaceutical Biol.
40 , 411-415 | 2002 |
| 42. A review on potentiality of medicinal plants as the source of new contraceptive principles. | R.Unny
M.P. Dobhal
R.S.Gupta | Phytomedicine
10 ,233 – 260 | 2003 |

Referees

1. **Prof B.C.Joshi, Ph.D., D.Sc.**
5 / 74, SFS, Agrawal Farms
Mansarovar, Jaipur- 302020 (India)

2. **Dr. Mahendra Kumar, Ph.D.**
Department of Chemistry
University of Rajasthan
Jaipur –302004 (India)